Department of Neurology
Faculty 2: Medicine – Clinical Medicine
Saarland University, Homburg/Saar, Germany

The Role of Acid Sphingomyelinase in Experimental Autoimmune Encephalomyelitis

Dissertation

A dissertation submitted in partial fulfillment of the requirements for the degree of Doctor of Philosophy

Faculty of Medicine

SAARLAND UNIVERSITY

2013

Submitted by: Laura Michelle Davies

Born on: 15 September 1984, in Edmonton, Canada

I dedicate this thesis to all those that supported me throughout my academic career: my mentors, my family and, most particularly, Christian, without whom none of this would have been possible.

Declaration

I hereby declare that this thesis is my own original work and effort. All experiments, except for those specified, were exclusively performed by me. The performance and evaluation of certain experiments, as listed in the text, were contributed by the following people (with no monetary reparation):

1. Prof. Dr. Erich Gulbins: ceramide clustering and acid sphingomyelinase analysis
2. Dr. Brian Henry: tight junction immunohistochemistry and Evans Blue quantification

The data presented here have not been submitted anywhere else for any award. Where other sources of information and help that have been used, they have been indicated and acknowledged.

Homburg, 26.02.2013

Laura Michelle Davies

Contents

Figures

Abbreviations

A	Absorption
aa	Amino acid
AEC	Amino-ethylcarbazol
APC	Allophycocyanin
ASM	Acid sphingomyelinase
Asm	Acid sphingomyelinase protein (mouse)
Asm$^{-/-}$	Acid sphingomyelinase genetic knockout
ATP	Adenosine triphosphate
BBB	Blood-Brain Barrier
bEnd.3	brain endothelialpolyoma middle T antigen transformed cell line
b.i.d.	Bi-daily
BM	Bone marrow
CD-4	Cluster of differentiation-4
CD-45	Cluster of differentiation-45
CD-49d	Cluster of differentiation-49d
CD-8	Cluster of differentiation-8
CFA	Complete Freud's Adjuvant
CFDA-SE	Carboxyfluorescein diacetate succinimidyl ester
Ci	Curie
CNS	Central nervous system
CSF	Cerebral spinal fluid
CST	Cytometer Setup and Tracking
Cy3	Indocarbocyanine
DAG	Diacylglycerol
dH$_2$O	Distilled water
DMEM	Dulbecco's Modified Eagle Medium
DMSO	Dimethyl sulfoxide
DTPA	Diethylenetriaminepentaacetic acid
EAE	Experimental autoimmune encephalomyelitis
EBV	Epstein-Barr virus
e.g.	*exempli gratia*, for example
EBD	Evans Blue Dye
EDTA	Ethylene diamine tetra acetic acid
etc.	*et cetera*
FACS	Fluorescence-activated cell sorting
FCS	Fetal calf serum
FITC	Fluorescein isothiocyanate
FIASMA	Functional Inhibitor of Acid Sphingomyelinase
g	Gram
g	*Gravity*
GMCSF	Granulocyte macrophage colony stimulating factor
Gy	Gray unit
h	hour
H$_2$O$_2$	Hydrogen peroxide
HBSS	Hanks Balanced Salt Solution
HEPES	4-(2-Hydroxyethyl)-1-piperazineethanesulfonic acid
H/S	HEPES/saline
HRP	Horse radish peroxidase
IgG	Immunoglobulin G

IgM	Immunoglobulin M
IL-2	Interleukin-2
IL-4	Interleukin-4
IL-17	Interleukin-17
IFNγ	Interferon gamma
IHC	Immunohistochemistry
i.p.	intraperitoneally
i.v.	intravenously
KO/ko	knock out
M	Molar
mg	Milligram
ml	Millilitre
min	Minute
mmol	Millimolar
MOG	Myelin oligodendrocyte glycoprotein
MRI	Magnetic resonance imaging
MS	Multiple sclerosis
ng	Nanogram
nm	nanometer
O.D.	Optical density
PBS	Phosphate buffer with salt
PCR	Polymerase chain reaction
PE	Phycoerythrin
PerCP	Peridinin-chlorophyll protein complex
PFA	Paraformaldehyde
p.i.	post-immunization
PLP	Myelin proteolipid protein
PMA	Phorbol-12-myristate-13-acetate
PPMS	Primary progressive MS
PRMS	Progressive relapsing MS
RGD	2-[[2-[[2-Amino-5-(diaminomethylideneamino)-pentanoyl]amino]-acetyl]amino]butanedioic acid
rpm	Revolution(s) per minute
RPMI	Roswell Park Memorial Institute
RRMS	Relapsing-remitting MS
RT	Room temperature
SCW	Spinal cord weight
SD	Standard deviation
sec	Second
SEM	Standard error of the mean
SJL	Swiss/Jackson Laboratory
SM	Sphingomyelin
Smpd1	Sphingomyelin phosphodiesterase-1 gene
SPMS	Secondary-progressive MS
TLC	Thin-layer chromatography
TNF-α	Tumor Necrosis Factor-α
U	Unit
μl	Microlitre
μm	Micrometer
UV	Ultraviolet
wk	Week

WT/wt   Wild type
% (v/v)   Volume/volume percentage solution
% (w/v)   Weight/volume percentage solution
ZO-1   Zona occludins-1

Abstract

Multiple sclerosis is one of the most common autoimmune disorders, and the leading cause of neurological disability in young adults in the Western world. Pathologically, multiple sclerosis begins with inflammatory infiltration into the brain and spinal cord, which leads to extensive demyelination, neuronal loss, and gliotic scars. The resultant central nervous system damage is responsible for the wide-ranging presentation of neurological symptoms such as motor and sensory deficits, vision impairment or ataxia. The active inflammatory foci are characterized by an initial infiltration of $CD4^+$ and $CD8^+$ T cells, which then orchestrate an inflammatory effector phase that ultimately leads to brain damage.

Central to this disease pathway is the adhesion of lymphocytes to endothelial cells and the ultimate migration of these lymphocytes from the peripheral circulation across the blood-brain barrier. The adhesion and transmigration of lymphocytes across the endothelium is a complex process involving interactions between complementary adhesion molecules on the surfaces of lymphocytes and endothelial cells. Following adhesion of the T cells to endothelial cells, the integrity of the blood-brain barrier is then compromised through breakdown of the tight and adherens junctions, which will then allow lymphocytes to migrate into the central nervous system parenchyma. Once the T cells have gained entry to the nervous system, they activate local microglia, which results in the production of vasoactive substances, chemokines, and cytokines that further attract additional peripheral leukocytes, triggering progressive damage.

The cause of multiple sclerosis, however, is not yet fully elucidated despite considerable knowledge about the pathophysiology of leukocyte infiltration. While multiple sclerosis is incurable, several drugs modify disease progression, including beta interferons, glatiramer acetate, mitoxantrone, FTY720, and the monoclonal antibody, natalizumab. These drugs have all been shown to reduce the number of relapses, however, none of these immunomodulating drugs can completely protect against disease progression. Furthermore, these drugs can have severe side effects, such as cardiotoxicity, liver damage, acute myeloid leukemia, and progressive multifocal leukoencephalopathy. Thus, the identification of novel targets and the development of therapeutic alternatives are of the utmost importance for the treatment of patients with multiple sclerosis.

In this study, we demonstrate that the acid sphingomyelinase/ceramide pathway plays a central role in the development of experimental autoimmune encephalomyelitis, the animal model of multiple sclerosis. Using this experimental model, we show that both genetic deficiency and pharmacological inhibition of acid sphingomyelinase by amitriptyline protects against the development of central nervous system inflammatory infiltrates and typical clinical symptoms. Acid sphingomyelinase converts sphingomyelin into ceramide in the outer layer of the cell membrane, which has previously been shown to form ceramide-enriched membrane platforms that serve to cluster receptors upon activation, thereby permitting and amplifying their signal transduction. Using bone marrow transplantation and adhesion assays, we demonstrate that ceramide mediates clustering of β-1 integrin on T lymphocytes upon contact with endothelial cells and thereby T lymphocyte adhesion. Inhibition of acid sphingomyelinase prevents lymphocyte adhesion and, thus, all subsequent pathophysiology including blood-brain barrier disruption, lymphocyte immigration into the parenchyma, and inflammation in the central nervous system. The functional blockade of the acid sphingomyelinase/ceramide system by the well-known antidepressant drug amitriptyline could be a novel therapeutic option for multiple sclerosis patients.

Zusammenfassung

Die Multiple Sklerose ist eine der häufigsten Autoimmunerkrankungen und gilt in der westlichen Welt als Hauptursache für neurologische Behinderungen bei jungen Erwachsenen. Aus pathologischer Sicht entsteht die Multiple Sklerose durch entzündliche Infiltrate im Gehirn und Rückenmark, die zu umfangreicher Demyelinisierung, Verlust von Nervenzellen und gliösen Narben führen. Die hierdurch verursachten Schäden des Zentralnervensystems sind für die weitreichenden neurologischen Symptome, wie motorische und sensorische Defizite, Sehstörungen oder Ataxie, verantwortlich. Kennzeichnend für die aktiven Entzündungsherde sind eine anfängliche Infiltration von CD4+ und CD8+ T-Zellen, die eine entzündliche Effektorphase einleiten und schließlich zur Schädigung des Zentralnervensystems führen.

Eine zentrale Rolle spielt bei der Krankheitsentstehung die Adhäsion von Lymphozyten an Endothelzellen sowie deren anschließende Migration aus dem peripheren Blutfluss über die Blut-Hirn-Schranke ins Zentralnervensystem. Die Adhäsion und Transmigration von Lymphozyten über das Endothel der Blut-Hirn-Schranke ist ein komplexer Prozess, bei dem Adhäsionsmoleküle auf der Oberfläche von Lymphozyten und Endothelzellen miteinander wechselwirken. Die initiale Bindung von T-Zellen an das Endothel beeinträchtigt durch einen Zusammenbruch von Tight Junctions und Adhärenzverbindungen die Barrierefunktion der Blut-Hirn-Schranke. Hierdurch wird den Lymphozyten die Einwanderung ins Hirnparenchym ermöglicht. Im Zentralnervensystem bewirken sie eine Aktivierung von lokalen mikroglialen Zellen, die wiederum die Produktion von vasoaktiven Substanzen, Chemokinen und Zytokinen fördern, weitere Leukozyten aus der Peripherie anziehen und somit zum Fortschreiten der Schädigung beitragen.

Die Ursache der Multiplen Sklerose ist jedoch, trotz der beträchtlichen pathophysiologischen Erkenntnisse über die Leukozyteninfiltration, noch nicht vollständig geklärt. Obwohl die Erkrankung nicht heilbar ist, gibt es verschieden Medikamente wie Betaferon, Glatirameracetat, Mitoxantron, FTY720 und den monoklonalen Antikörper Natalizumab, die ihren Verlauf beeinflussen. Für alle diese Medikamente wurde gezeigt, dass sie die Anzahl der Schübe verringern, ein Fortschreiten der Krankheit jedoch nicht komplett verhindern können. Des Weiteren können bei der Einnahme der oben genannten Medikamente ernste Nebenwirkungen wie Kardiotoxizität, Leberschäden, akute myeloische Leukämie und eine progressive multifokale Leukenzephalopathie auftreten. Aus diesen Gründen sind die

Erkennung von neuen Angriffspunkten und die Entwicklung therapeutischer Alternativen von äußerster Wichtigkeit für die Behandlung von Patienten mit Multipler Sklerose.

In dieser Studie zeigen wir, dass der Sphingomyelin/Ceramid-Reaktionsweg eine zentrale Rolle in der Entwicklung der Experimentellen Autoimmunen Enzephalomyelitis, dem Tiermodel der Multiplen Sklerose, spielt. Anhand dieses experimentellen Modells wird demonstriert, dass sowohl der genetische Mangel als auch die medikamentöse Hemmung der sauren Sphingomyelinase durch Amitriptylin vor der Entstehung entzündlicher Infiltrate im Zentralnervensystem und der Entwicklung der typischen klinischen Symptome schützen. Die saure Sphingomyelinase spaltet Sphingomyelin in der äußeren Zellmembran, wodurch Ceramid entsteht. In Studien wurde bereits gezeigt, dass die hierdurch gebildeten Ceramid-angereicherten- Plattformen zur Clusterbildung aktivierter Rezeptoren dienen, wodurch deren Signaltransduktion ausgelöst und verstärkt wird.

Mit Hilfe von Knochenmarkstransplantation und Adhäsionsassays zeigen wir, dass Ceramid die Bildung von β-1 Integrin-Clustern auf T-Lymphozyten, nach deren Kontakt mit Endothelzellen, vermittelt und damit die Lymphozytenadhäsion ermöglicht. Entsprechend verhindert eine Hemmung der sauren Sphingomyelinase die Adhäsion und damit alle folgenden Pathomechanismen, wie die Schädigung der Blut-Hirn-Schranke, die Einwanderung von Lymphozyten in das Hirnparenchym und die Entzündung des Zentralnervensystems. Die funktionelle Blockade des Sphingomyelin/Ceramid-Systems durch das bekannte Antidepressivum Amitriptylin könnte eine neue Therapieoption für Patienten mit Multipler Sklerose darstellen.

1 Introduction

1.1 MS overview

Multiple sclerosis (MS) is the most common inflammatory disorder of the central nervous system (CNS) and a leading cause of disability in young adults (Milo and Kahana, 2010). It is estimated that the total number of people worldwide living with this disorder is 2-2.5 million. MS was first described by Jean-Martin Charcot (Fig. 1.1) in 1868 and was, in fact, called Charcot disease until 1921 (Clanet, 2008). Throughout his career (1848-1893), Charcot saw around 30 cases of MS and thought that it was a rare disorder, with a propensity for females, though he noted that the incidence was increasing with improved diagnostic accuracy.
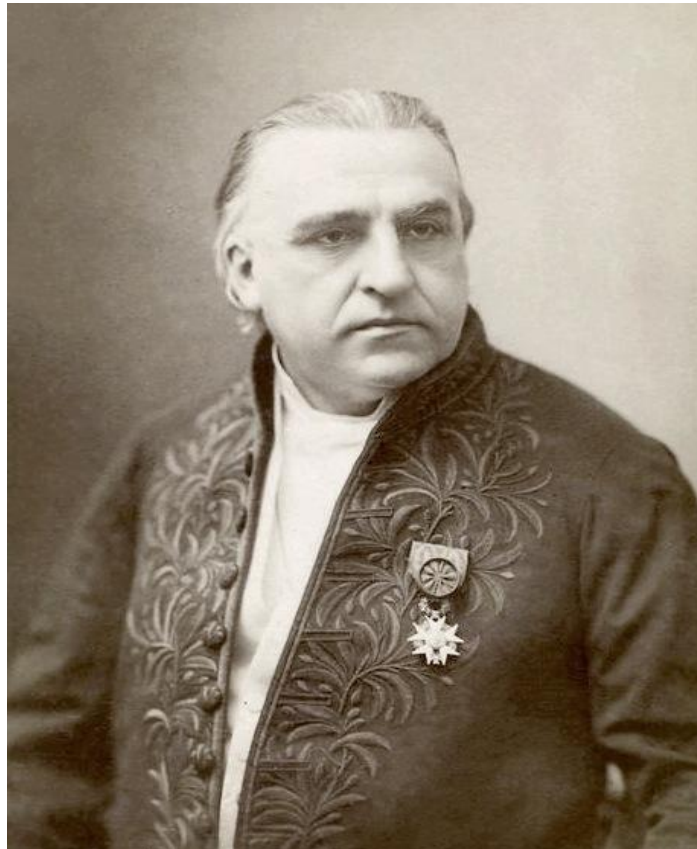
Figure 1.1 Jean-Martin Charcot (1825-1893). Images from the History of Medicine, National Library of Medicine (public domain).

Since its first description in the mid-1800's as a rare neurologic condition, the diagnosis of MS has significantly increased to an incidence of 0.7-8.7 per 100,000/year and a prevalence of 1-287 per 100,000 people, depending on geographic location (Rosati, 2001). The pattern of disease is unevenly distributed throughout the world and increases progressively with

geographic latitude: its prevalence varies from <5 cases per 100,000 people in tropical areas/Asia and >100-200 cases per 100,000 people in temperate regions including Canada, the United States, northern Europe and New Zealand (Fig. 1.2).
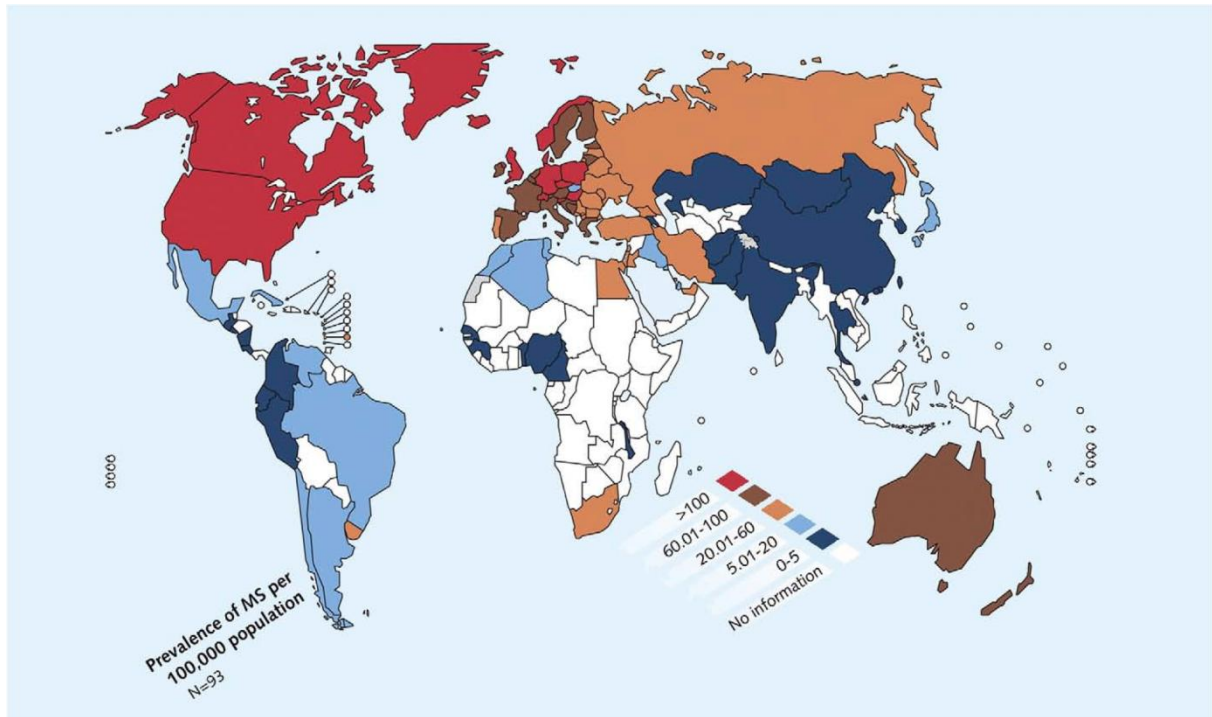
Figure 1.2 Multiple sclerosis prevalence geographic distribution (Milo and Kahana, 2010).

There is also uneven gender distribution; as noted by Charcot, there is a higher prevalence of females with MS worldwide (female/male ratio around 2:1) and an even greater difference has been noted in select populations, specifically Canada where the female/male ratio is 3:1 (Orton et al., 2006).

Clinical symptoms typically present between 20-50 years of age, with a peak at 30 years of age. MS patients present with a variety of neurological signs and symptoms attributed to white matter lesions disseminated in time and space, and may occur in sudden attacks or as insidious neurologic progression. Common presenting symptoms can include paresthesias, incoordination, motor weakness, monocular visual disturbances (optic neuritis), diplopia, vertigo, and dizziness (Compston and Coles, 2008). These symptoms may also be accompanied by other signs including fatigue, sexual dysfunction, urinary retention or urgency, pain, cognitive dysfunction, ataxia or Lhermitte's phenomenon (an electrical sensation running down the back to the limbs on neck flexion). This list is not exhaustive, and patients have a large variability in presentation.

The clinical course of MS is highly variable. Approximately 85% of patients will present with a relapsing-remitting (RRMS) course characterized by sudden attacks of neurological signs and symptoms followed by complete or partial recovery lasting from days to months and separated by periods of stable neurological condition without clinical disease activity (Milo and Kahana, 2010). The other 10-15% will present with a primary-progressive (PPMS) course characterized by a steady accumulation of neurological disability from disease onset. Some of these patients may have superimposed relapses, which is then classified as a progressive-relapsing (PRMS) course. Eventually, 65% of patients originally presenting with RRMS will convert to a secondary progressive (SPMS) disease course (Compston and Coles, 2008). The mean reduction in life expectancy is 5-10 years, representing a median time to death of 30 years from disease onset (Bronnum-Hansen et al., 2004). However, it is important not to forget the impact of this disease on patient mental health, as it has been demonstrated that patients with MS have an increased lifetime frequency of depression of up to 50% and a greater risk of suicide (Minden and Schiffer, 1990).

The diagnosis of MS is based on an evolving set of criteria, called the McDonald Criteria, most recently updated in 2011 (Polman et al., 2011). This clinical guideline takes into account medical history, clinical neurological exam, MRI, visual evoked potential and spinal fluid analysis. Patients are assessed for past or current presence of an attack, defined as patient-reported or objectively observed events typical of an acute inflammatory demyelinating event in the CNS, current or historical, with duration of at least 24 hours, in the absence of fever or infection. When the patient has experienced 2 or more attacks with objective clinical evidence of a lesion and dissemination in space demonstrated by ≥ 1 T2 lesion in at least 2 of 4 MS-typical regions of the CNS (periventricular, juxtacortical, infratentorial, or spinal cord), and all other diagnoses have been ruled out, a diagnosis of MS can be made with reliable accuracy. When there is only evidence of 1 attack, or there is insidious neurological progression suggestive of MS, then the criteria to demonstrate dissemination in space and time as well as presence of positive CSF findings, including isoelectric focusing evidence of oligoclonal bands and/or elevated IgG index, must be utilized to make a diagnosis. It should be noted that before a definite diagnosis of MS can be made, at least 1 attack must be corroborated by findings on neurological examination, visual evoked potential response in patients reporting prior visual disturbance, or MRI consistent with demyelination in the area of the CNS implicated in the historical report of neurological symptoms.

The cause of MS is not conclusively known, though it is believed to be multifactorial in nature. The main factors thought to contribute to MS are environment, genetics, and infection. A number of environmental factors have been implicated in an increased risk of MS including organic solvents and dental amalgam, but the factor most likely associated with MS susceptibility is sunlight exposure mediating vitamin D synthesis and ultraviolet radiation. This hypothesis would generally explain the geographical distribution, as the more northern cultures would have less sun exposure and thus less vitamin D synthesis. While vitamin D supplementation has been shown to be inversely associated with MS risk and will even suppress EAE in an experimental model, it is not certain whether it is the vitamin D levels alone or the combination of vitamin D with UV exposure that is protective (Milo and Kahana, 2010).

Epstein-Barr virus (EBV) infection has also been implicated in the pathogenesis of MS and, in fact, follows a similar geographic distribution. Populations with early EBV exposure (a high proportion of seropositivity pre-adolescence) have a decreased risk of MS compared to populations with late exposure (Ascherio and Munger, 2007). There is also evidence to implicate genetic factors in MS pathogenesis; twin studies have shown a concordance rate of 25-30% and an index of heritability of 0.25-0.76 in monozygotic twins (Hawkes and Macgregor, 2009). Furthermore, about 20% of MS patients have at least one affected relative and the risk for developing MS in first-degree relatives is increased 3.4-5.13% (Dyment et al., 1997). Likewise, there is a 10-fold increased risk in children from parents who both have MS. These studies point to a genetic susceptibility, and not a mendelian inheritance pattern, but the precise genes involved have not yet been elucidated. Based on the current research, the pathogenesis of MS is likely multifactorial and dependent upon environmental factors including vitamin D, UVR, EBV infection and a genetic predisposition.

Although there is no cure for MS, there are a number of disease-modifying therapies in use that can mitigate progression of the disease. These agents include glatiramer acetate (Johnson et al., 1995), interferon (IFN) β-1a (Jacobs et al., 1996), IFN β-1b (Paty and Li, 1993), the monoclonal antibody, natalizumab (Polman et al., 2006) and, more recently, the sphingosine-1-phosphate (S1P) receptor modulator, FTY720 (Kappos et al., 2010). However, these drugs can have severe side effects associated with their usage including bradycardia, and resultant asystole, in the case of FTY720 (Espinosa and Berger, 2011) and progressive multifocal leukoencephalopathy (PML) in the case of natalizumab (Sorensen et al., 2012). These severe

conditions and the numerous other negative ramifications including influenza symptoms, opportunistic infections, liver damage, etc. limit the ability to use these drugs in the clinical setting and prompts the need to continue the search for more effective treatment strategies with fewer side effects.

1.2   Pathophysiology

MS is generally thought to be an immune-mediated disorder, though the exact sequence of events that leads to demyelination is not completely understood. There is a large degree of heterogeneity in clinical presentation, MRI and pathologic progression such that one underlying mechanism may not be fully responsible, but instead a number of factors that influence the outcome. Chronic MS lesions are characterized by the demyelinated plaque, consisting of a well-demarcated hypocellular area with loss of myelin, relative preservation of axons and astrocytic scars (Noseworthy et al., 2000). These chronic lesions are often round or oval, and occasionally follow the path of blood vessels creating what are called "Dawson's fingers" (Fig 1.3).
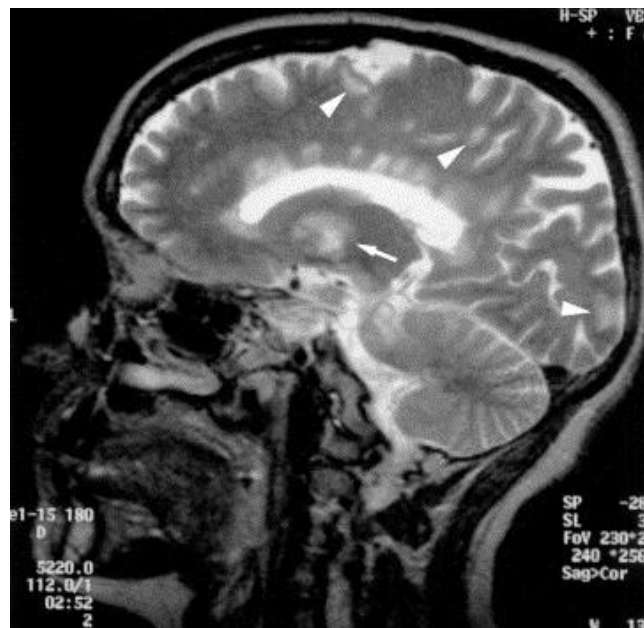
Figure 1.3 Dawson's Fingers on MRI. Sagittal T2-weighted image in a patient with long-standing MS showing multiple periventricular plaques (Dawson's fingers) adjacent to the corpus callosum. Thalamus (arrow) and juxtacortical white matter (arrowheads) are also affected (Pretorius and Quaghebeur, 2003).

Inflammatory infiltrates in the CNS are generally perivascular with some parenchymal diffusion and are primarily composed of macrophages and lymphocytes (Noseworthy et al.,

2000). However, in order to understand the underlying mechanism of MS, it is important to assess the role of the blood-brain barrier, lymphocyte adhesion and subsequent transmigration.

Since the late 1800's, the brain has been considered a privileged organ; insulated from the rest of the body. Starting from the early work of Paul Ehrlich, a German physician, who reported in 1885 that the brain and spinal cord did not stain when a dye was injected into the vascular system of mice (Ribatti et al., 2006). In 1900, Lewandowsky introduced the term "blood-brain barrier" (BBB) following experiments where dye was injected into the cerebrospinal fluid (CSF) resulting in parenchymal staining, thus overcoming some "barrier". Further work in the early 1920's by Shirai in Japan and Murphy and Sturm with rat sarcoma, revealed that the brain was protected from normal immune responses, later termed "immunological privilege" by Billingham and Boswell (Galea et al., 2007). This privilege allowed tissue grafts, bacteria, viruses and vectors to evade immune recognition when delivered into the brain parenchyma. However, although peripheral immune access is certainly restricted and well controlled, we now know that the central nervous system (CNS) is capable of and subject to inflammatory responses to a variety of insults (Rivest, 2009).

The CNS is able to maintain its immuno-privileged status, mostly due to restriction of peripheral leukocyte trafficking from the periphery to the CNS through the BBB. The BBB (Fig 1.4) is composed of endothelial cells, astrocytes, basement membrane and junctional proteins (Persidsky et al., 2006).
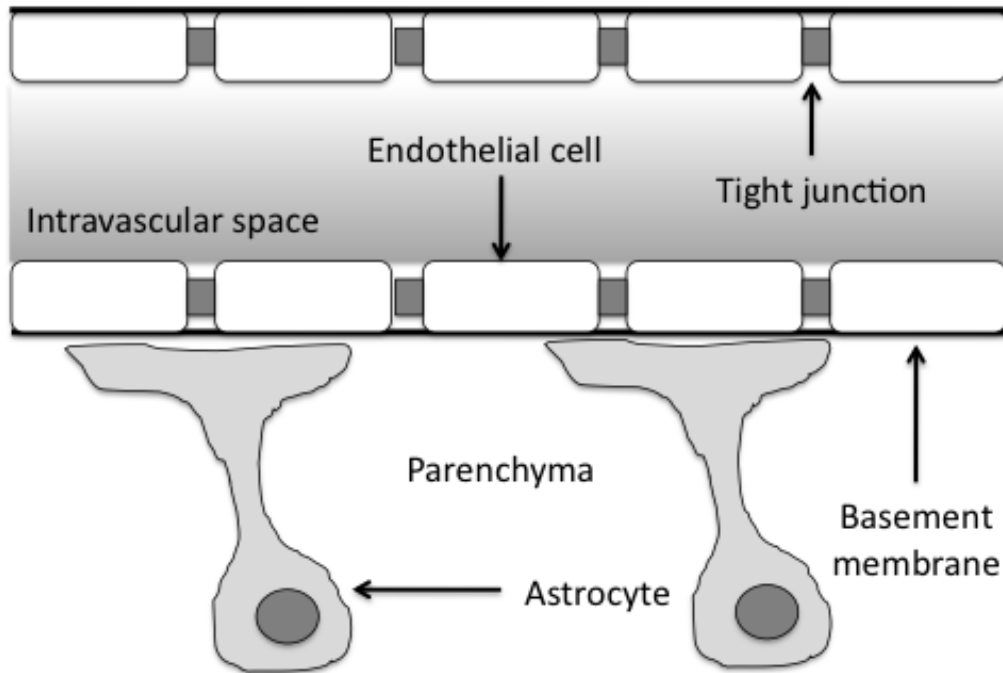
Figure 1.4 Schematic of blood-brain barrier (BBB).

Astrocytes are an integral component of the BBB and envelop >99% of the BBB endothelium (Hawkins and Davis, 2005). The presence of tight junctions is also a key feature of an intact BBB, and includes: occludin, the claudins and junctional adhesion molecules (Persidsky et al., 2006). Under normal conditions, leukocyte entry is kept to a low level because autoreactive naïve T cells undergo negative selection and apoptosis. However, in MS, for whatever reason, these autoreactive cells do not apoptose and have the potential to attack the CNS, effecting autoimmune responses against myelin components through molecular mimicry, bystander activation and epitope spreading (Fujinami et al., 2006).

In order to study the pathologic mechanisms behind MS, scientists have assessed an animal model designated as experimental autoimmune encephalomyelitis (EAE). Since its discovery in 1933 (Rivers et al., 1933), it has been used to replicate MS and acute disseminated encephalomyelitis (ADEM) in a variety of animal models, particularly rodents. The EAE model consists of two phases: 1) T cell priming and activation in the periphery, and 2) an effector phase with migration of leukocytes across BBB, local reactivation and invasion into CNS parenchyma (Becher et al., 2006). The migration of T cells across the BBB is a complex interaction between adhesion molecules on the surface of lymphocytes and endothelial cells

(Engelhardt and Ransohoff, 2005). T cell migration is thought to proceed with the following progression (Fig 1.5):

1.) T cell rolling mediated by α-4 integrins and P-selectin glycoprotein ligand-1 (Kerfoot and Kubes, 2002)

2.) Homeostatic chemokines (e.g. CCL19 and CCL21) produced by endothelial cells likely mediate T cell activation through G-protein coupled receptors (GPCRs) (Alt et al., 2002)

3.) Firm adhesion via ICAM-1 and VCAM-1 on endothelial cells interacting with LFA-1 and α4β1 on lymphocytes (Laschinger et al., 2002).

4.) T cell crawling and transmigration (Schenkel et al., 2004).

5.) CD4+ T cells accumulate in perivascular spaces, and encounter specific antigens on antigen presenting cells (APCs) which reactivates the lymphocytes (Greter et al., 2005).
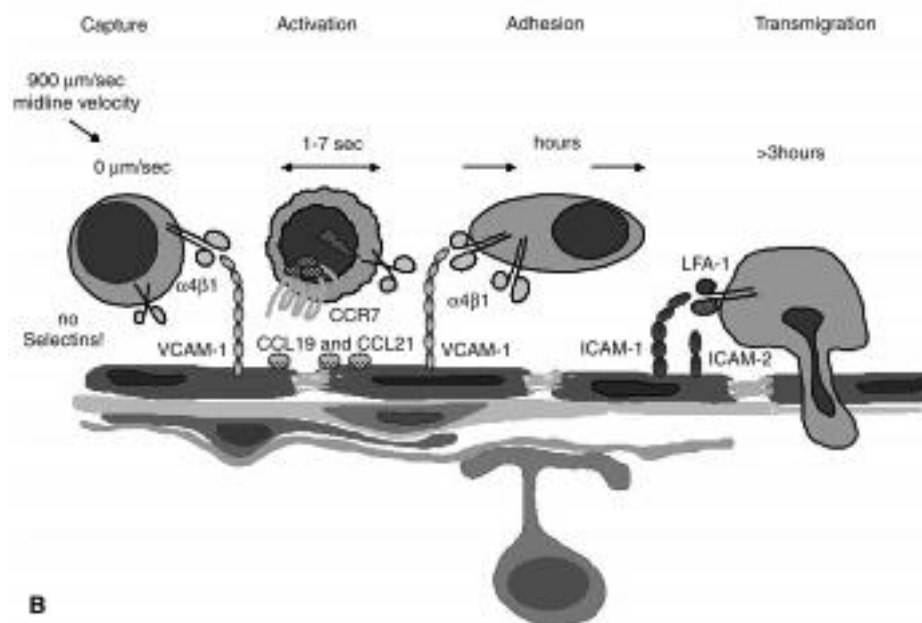
Figure 1.5 Schematic of lymphocyte adhesion/transmigration. The multi-step model of lymphocyte adhesion and transmigration across the blood-brain barrier endothelium in spinal cord white matter (Engelhardt, 2006).

T cells that have crossed into the CNS parenchyma then activate local microglia which produce vasoactive substances, chemokines and cyto- and myelinotoxic cytokines attracting peripheral lymphocytes and damaging brain tissue (Frohman et al., 2006). Cytokines including TNFα, IL-1β, IL-2, LTα, LTβ and IFNγ are upregulated in the cerebrospinal fluid

(CSF) and brain tissue of MS patients (Kunz and Ibrahim, 2009) and some of these cytokines modulate phospholipid and sphingolipid metabolism (Plo et al., 1999).

1.3 Acid sphingomyelinase

Sphingomyelinases are a family of enzymes that catalyze the breakdown of sphingomyelin into ceramide by cleavage of the phosphorylcholine linkage (Fig 1.6). The first sphingomyelinase was discovered in 1940 by Thannhauser and Reichel (Thannhauser S J, 1940), and several more have been discovered since then, differing in tissue distribution and pH optimum. Acid sphingomyelinase (Asm) was first clearly described by Gatt (Gatt, 1963) and the deficiency of which was subsequently found to be responsible for Niemann-Pick disease (Type A and B); a rare, autosomal recessive inherited lysosomal storage disorder (Brady et al., 1966). The gene for Asm is called SMPD1, and is found on chromosome 11p15.4; the gene encodes a 629 amino acid polypeptide (Schuchman et al., 1992). It has both a lysosomal form (75 kDa) and a secreted form (57 kDa) (Ferlinz et al., 1994).
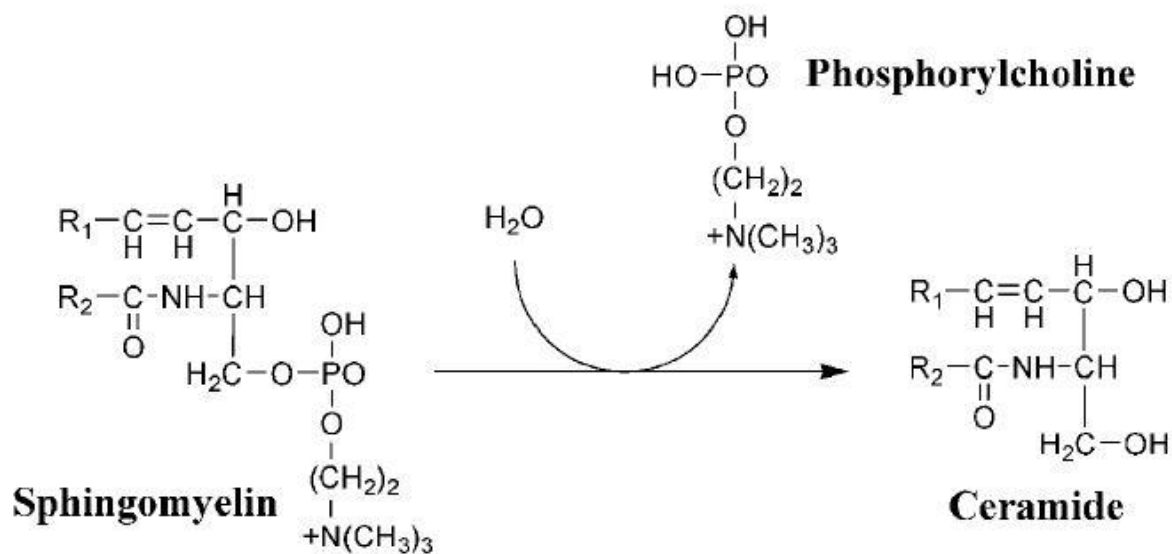
Figure 1.6 Formation of ceramide from sphingomyelin via acid sphingomyelinase (Seto et al., 2004). During the creation of ceramide from sphingomyelin, a phosphorylcholine is released as a by-product.

Asm is a zinc metalloprotein and the secreted form requires exogenous zinc for full activity (Schissel et al., 1996) as well as removal of the terminal cysteine residue (Qiu et al., 2003). Asm *in vitro* has an optimum pH of 4.5-5, and some studies have shown acidified microenvironments at the cell surface linking these microenvironments and lipid

microdomains, which is where Asm is active (Ro and Carson, 2004). The secreted form of Asm is able to be fully active in LDL particles at physiologic pH (Schissel et al., 1998). Asm releases ceramide in the outer layer of the cell membrane from sphingomyelin (major pathway of ceramide generation, see Fig 1.7 and 1.8) allowing formation of ceramide-rich microdomains which fuse to form rafts which can re-organize cell signaling proteins, cluster receptor molecules and amplify signals (Gulbins and Li, 2006).

Palmitoyl-CoA + Serine

| *Serine-palmitoyl transferase*

3-Ketosphinganine

| *3-Ketosphinganine reductase*

Sphinganine

| *Ceramide synthase*

Dihydroceramide

| *Dihydroceramide desaturase*

Sphingo-
myelin ⇌ (Sphingo-myelinases / Sphingomyelin synthase) ⇌ Ceramide ⇌ (Ceramidase / reverse Ceramidase activity) ⇌ Sphingosine
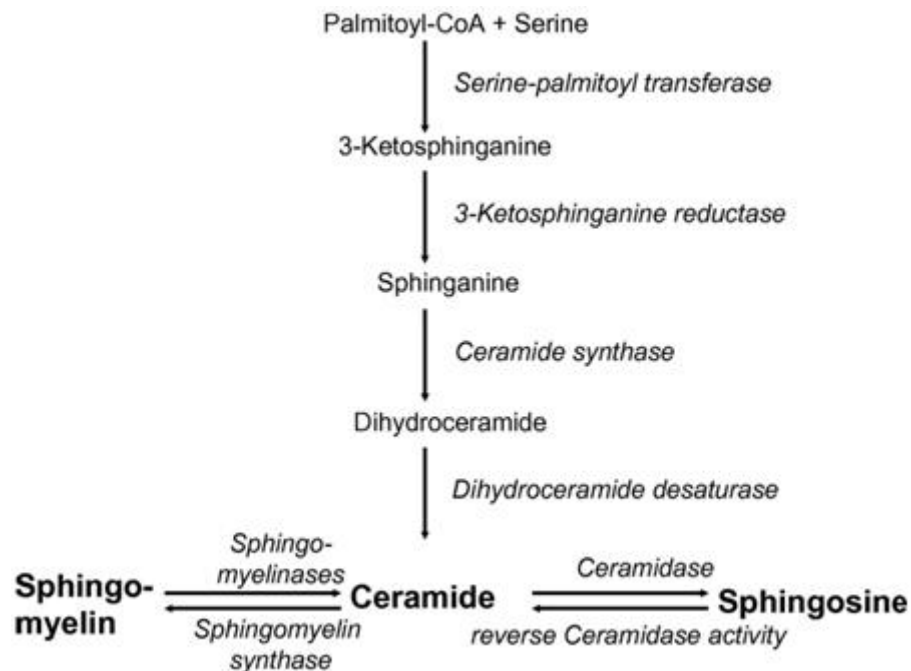
Figure 1.7 Ceramide pathway (Henry et al., 2011). Ceramide can be synthesized *de novo* from palmitoyl-CoA or through the conversion of sphingomyelin via sphingomyelinase. Ceramide can also be created via ceramidase (salvage pathway).

Activation of Asm, and subsequent release of ceramide, was demonstrated after stimulation with numerous interventions including CD95, TNF receptor, irradiation, UV-light, and treatment with chemotherapeutic drugs (doxorubicin, cisplatin, gemcetabine). However, it is also activated upon stimulation with CD28, CD40, CD14, CD5 and LFA-1. CD40 ligation results in Asm moving from internal cell stores to the extracellular surface of the plasma membrane where it acts to produce ceramide from sphingomyelin, resulting in ceramide rich domains (Grassme et al., 2002a). Furthermore, genetic deficiency of Asm prevents CD40 clustering and cell signaling pathways, a result which can also be produced by the neutralization of ceramide (Grassme et al., 2002b). Asm is also activated by stimulation of T cells with CD28 and results in impaired IL-2 secretion when cells are genetically deficient (Stoffel et al., 1998). Asm inhibition, whether through genetic deficiency, pharmacologic

inhibition or siRNA, provides protection against stimuli that would normally cause apoptosis including ischemia (Yu et al., 2000), radiation (Paris et al., 2001), and chemotherapy (Dimanche-Boitrel et al., 2005).

The majority of pharmacologic inhibitors of Asm belong to a class of drugs called "FIASMAs" (Functional inhibitor of acid sphingomyelinase) as defined by Kornhuber et al. in 2010 (Kornhuber et al., 2010). These drugs are weak organic bases and include desipramine (Kolzer et al., 2004), fluoxetine, sertraline and amitriptyline (Kornhuber et al., 2008), as well as many others. It is thought that these drugs inactivate Asm indirectly by causing the release of the enzyme from the inner membrane of the lysosome (Kolzer et al., 2004) resulting in inactivation through proteolytic degradation (Hurwitz et al., 1994).

1.4 Sphingolipids in Multiple Sclerosis

Much of what we know in this field has only been discovered in the last 15 years and remains a veritable treasure trove for future studies and developments. However, although there is still much to learn, progress in the understanding and treatment of multiple sclerosis has already taken place. From the clinical setting it has been shown, through lipid microarray analysis, the presence of anti-sphingomyelin antibodies in the CSF of MS patients (Kanter et al., 2006). The role of sphingolipids in multiple sclerosis is complex, acting on diverse mechanisms such as apoptosis (Jana and Pahan, 2007), T cell trafficking (Goetzl and Graler, 2004), astrogliosis (Wu et al., 2008), and receptor clustering (Grassme et al., 2002b).

1.4.1 Leukocyte activation and trafficking

Leukocyte activation is a crucial event in protective and adaptive immunity and is involved in the maintenance of self-tolerance. Although entry of leukocytes into the CNS is low under normal circumstances, pathologic conditions can increase trafficking. During T cell activation, antigen is processed and presented by antigen presenting cells to T lymphocytes through MHC molecules, which bind to the T cell receptor. The receptor ligation causes formation of lipid rafts and aggregation of co-stimulatory ligands resulting in a structural dependent/associated mechanism for promoting immune cell signaling (Luo et al., 2008). Specifically, stimulation of T cells via CD28 (an important co-stimulatory receptor) causes the activation of Asm and release of ceramide (Boucher et al., 1995).

15

LFA-1, a key adhesion molecule, also triggers release of ceramide, possibly through Asm (Rosenman et al., 1993). Ceramide released by neutral sphingomyelinase (NSM) is also involved in the stimulation of lymphocytes via the adhesion molecule, L-selectin (Phong et al., 2003). Additionally, the production of ceramide in endothelial cells triggers upregulation of Weibel-Palade bodies (Bhatia et al., 2004) resulting in increased expression of P-selectin (Babich et al., 2009), which promotes adhesion of leukocytes to endothelial cell layers (Burns et al., 1999). These studies show that the sphingolipid pathway is highly involved in the activation and adhesion of leukocytes.

Interestingly, treatment of MS patients with fluoxetine, a functional inhibitor of Asm (Kornhuber et al., 2008), has been shown to reduce the MRI lesion progression in a clinical trial (Mostert et al., 2008). Furthermore, it has been demonstrated that the S1P receptor is important for emigration of lymphocytes from both thymus and peripheral lymphoid organs (Goetzl and Rosen, 2004). FTY720 downregulates $S1PR_1$ expression in lymphocytes by inducing internalization, and degradation of the receptor, thereby resulting in lymphocyte sequestration (Oo et al., 2011). Kappos et al. (Kappos et al., 2006) reported that administration of FTY720 in MS patients reduced the number of lesions on MRI and clinical disease severity.

1.4.2 Pro-inflammatory mediators

Many chronic CNS diseases, acute CNS injuries, some psychiatric disorders and aging CNS are associated with a progressively spreading inflammation and marked oxidative stress (Lucas et al., 2006). Specifically, chronic neuroinflammatory disorders (such as multiple sclerosis) are associated with elevated levels of proinflammatory cytokines (Kunz and Ibrahim, 2009), chemokines, cell adhesion molecules, proinflammatory enzymes such as inducible nitric oxide synthase (iNOS) and cyclooxygenase (Jana and Pahan, 2010). This chronic neuroinflammation results in sustained release of inflammatory mediators, which perpetuates a vicious cycle of glial activation and further release of factors. These inflammatory mediators (cytokines, eicosanoids, etc.) and reactive oxygen species are largely responsible for the degeneration of neuronal cells (Barth et al., 2012). The proinflammatory molecule, TNFα, has been highly associated with neuroinflammatory diseases, especially MS (Bielekova and Martin, 2004). Stimulation of the TNFα receptor activates Asm (Schneider-Brachert et al., 2004) and Mg^{2+}-dependent NSM, and the resulting sphingomyelin hydrolysis,

rather than de novo synthesis, was the predominant source of ceramide increases in a primary cortical neuronal cell line (Barth et al., 2012).

Additionally, persistent glial activation and increased proinflammatory cytokine levels lead to BBB disruption, transvascular leakage and lymphocyte migration through upregulation of cell adhesion molecules (ICAM-1, VCAM-1 and selectin) expressed on BBB endothelium. Thus, regulation of the release of these factors could lead to promising therapies in the field of neuroinflammation.

2 Aim of this work

While much progress has been made in the development of drugs for MS, it is still not possible to completely control MS and many of the currently available drugs have serious side effects that prohibit their use in some patients. It is of the utmost importance that we continue to search for treatments that will prevent relapses without the associated side effects. To this end, we chose to study the Asm enzyme due to the role of ceramide (the enzymatic end-product) in receptor clustering and the ability to inhibit Asm activity with pharmacologic agents, specifically amitriptyline, that have minimal side effects and have been in clinical use for more than 50 years.

The aim of this study was to identify the role of Asm in MS pathophysiology and elucidate the cellular and molecular mechanisms mediated through this enzyme pathway. In detail, we aimed to answer the following questions:

1. How does loss of Asm function, either through genetic knockdown or pharmacologic inhibition, affect clinical outcome?
2. How does Asm affect lymphocyte and endothelial cell activity?
3. How does Asm affect the molecular pathways and expression within these cell types?

3 Materials and Methods

3.1 Materials

3.1.1 Instruments

Instrument	Source
Accu-Jet Pipette Controller	BrandTech Scientific, Essex, USA
Autoclave V-150, V-2540EL	Systec, Wettenberg, Germany
Axiovert 25 inverted microscope	Carl Zeiss Microscopy, Jena, Germany
Biofuge 13 Centrifuge	Heraeus, Hanau, Germany
Eclipse TS100 Inverted Microscope	Nikon Instruments Inc., Melville, USA
Electric Heatable, Forceps for Safer Transfer of Tissue Specimens Leica EG F	Leica Microsystems Nussloch GmbH, Nussloch, Germany
Eclipse E600 fluorescence microscope	Nikon, Alzenau, Germany
Epson perfection V700 photo scanner	Epson, Munich, Germany
FACSCanto™ II Flow Cytometer	BD Biosciences, San Jose, USA
Fixed-angle rotor for Optima MAX series ultracentrifuge MLA-130, TLA-100.3, TLA-100	Beckman Coulter, Fullerton, USA
Forced-air laboratory freezer	Liebherr, Ochsenhausen, Germany
Forced-air laboratory refrigerator	Liebherr, Ochsenhausen, Germany
General Rotator, STR4	Stuart Scientific, Staffordshire, UK
HERAcell CO_2 incubator	Heraeus, Hanau, Germany
HERAcell 150i CO2 Incubator	Thermo Scientific, Langenselbold, Germany
Heraeus HERAsafe HS 12 biological safety cabinet (Class II)	Heraeus, Hanau, Germany
Heraeus function line heating and drying ovens	Heraeus, Hanau, Germany
HERAfreeze -86C freezer	Heraeus, Hanau, Germany
Ice machine	Eurfrigor Ice Makers Srl, Lainate, Italy
Incubation hood TH30 and Universal shaker SM30	Carl Roth GmbH, Karlsruhe, Germany
Laboratory balance ALS120-4, EW4200, EW420	Kern & Sohn, Balingen, Germany
Laboratory centrifuge SIGMA 4K15C	Sigma Laborzentrifugen GmbH, Osterode am Harz, Germany

Laboratory pH meter InoLab pH 720	WTW, Weilheim, Germany
Leica SM 2000 R Sliding Microtome	Leica Microsystems Nussloch GmbH, Nussloch, Germany
Leica TP1020 Tissue Processor	Leica Microsystems Nussloch GmbH, Nussloch, Germany
Leica EG1150C Cold plate	Leica Microsystems Nussloch GmbH, Nussloch, Germany
Leica EG1150 H Heated Paraffin Embedding Module	Leica Microsystems Nussloch GmbH, Nussloch, Germany
Leica TCS SP5 Confocal microscope	Leica Microsystems Nussloch GmbH, Nussloch, Germany
Leica TCS SL software program, version 2.61	Leica, Mannheim, Germany
Liquid scintillation counter	Beckman Coulter, Krefeld, Germany
Micro-plate reader	TECAN, Sunrise Remote, Männedorf, Switzerland
Magnetic stirrer	Ika-Combimag RCO, Namur, Belgium
Microscope Zeiss Axio Scope	Carl Zeiss, Göttingen, Germany
MLA-130 Rotor, Fixed Angle, Titanium for Ultracentrifuge	Beckman Coulter, Brea, USA
Multiband UV table	Peqlab, Karlsruhe, Germany
Multipette® plus	Eppendorf, Hamburg, Germany
Nanodrop ND-1000 spectrophotometer	Peqlab, Karlsruhe, Germany
Nuaire IR AutoFlow NU-2700E Water-Jacketed CO_2 Incubator	Plymouth, MN
Pipette PIPETMAN P2, P20, P200, P1000	Gilson, Villiers le Bel, France
Pipette Single-Channel 2µl-20µl, 10µl-100µl, 100µl-1,000µl	Eppendorf, Hamburg, Germany
Pipette Pipetus	Hirschmann, Eberstadt, Germany
Platform shaker Duomax 1030	Heidolph, Schwabach, Germany
Precision Balance scale	Sartorius, Goettingen, Germany
Sigma 4K10 bench top centrifuge	Sigma Laborzentrifugen GmbH, Osterode am Harz, Germany
SmartSpecÔ3000 Spectrophotometer	Bio-Rad Laboratories, Hercules, USA
Sonopuls HD2070	Bandelin Electronic, Berlin, Germany
Stretching Table OTS 40	MEDITE GmbH, Burgdorf, Germany
Super High pressure Mercury Lamp Power supply	Nikon, Alzenau, Germany

Thermoblock TDB-120	BioSan, Riga, Latvia
Thermomixer Comfort	Eppendorf, Hamburg, Germany
Ultra-pure water purification system PURELAB Ultra	ELGA, Celle, Germany
Ultracentrifuge Optima MAX 130,000 rpm	Beckman Coulter, Fullerton, USA
UV/visible spectrophotometer Ultrospec3100pro	Amersham Biosciences, Munich, Germany
Vortex Genie 2	Scientific Industries, Bohemia, USA
Vortex-Shaker Reax 2000	Heidolph, Schwabach, Germany
Water bath	Köttermann GmbH & Co KG, Hänigsen, Germany

3.1.2 Experimental materials

Material	Source
Assistent® 12mmø Microscope cover glasses	Glaswarenfabrik Karl Hecht KG, Sondheim, Germany
BD Falcon™ FACS tubes	Becton, Dickinson and Company, Heidelberg, Germany
BD Falcon™ Serological pipet, 5ml, 10ml, 25ml	Becton, Dickinson and Company, Heidelberg, Germany
BD Plastipak syringe, 1ml	Becton, Dickinson and Company, Heidelberg, Germany
Biosphere filter tips 10ml, 100ml, 1000ml	Sarstedt, Nürnbrecht, Germany
Bottle Top Filter 500ml, 0.22mm	Sarstedt, Nürnbrecht, Germany
Cell strainer with 70µm nylon mesh, Sterile	BD Biosciences, San Jose, USA
Chamber slide	VWR, Darmstadt, Germany
Combination cap	Fresenius Kabi AG, Homburg, Germany
Combitips (plus) 5ml, 10ml, 12.5ml	Eppendorf, Hamburg, Germany
Cover glasses	Assistant, Sondheim, Germany
Cover slips 10 ´ 10 mm	Marienfeld, Lauda-Königshofen, Germany
Cryopure tubes for cell freezing	Sarstedt, Nümbrecht, Germany
CST beads	BD Biosciences, Durham, USA
Dako pen	Dako, Glostrup, Denmark

Falcon round-bottom tubes 14 ml	BD Biosciences, San Jose, USA
Filter cassette	Perkin Elmer Inc., Rodgau, Germany
Filter mat	Perkin Elmer Inc., Rodgau, Germany
Glass fibre filter 90x120 mm	Perkin Elmer Inc., Rodgau, Germany
Homogenizer	Hartenstein, Würzburg, Germany
Immersion Oil "Immersol" 518 F fluorescence free	Carl Zeiss, Göttingen, Germany
Isoflurane	Baxter, Unterschleißheim, Germany
Laboratory glassware	Schott, Mainz, Germany
Luerlock syringe 1 ml	BD Biosciences, Durham, USA
Microscope slides 76 ´ 26 mm	Gerhard Menzel, Braunschweig, Germany
Multiwell cell culture plate, 6well, 12well, 24well, 48well, 96well	Falcon, Becton Dickinson labware, Franklin Lakes, NJ
Nalgene "Mr Frosty" freezing container	Thermoscientific, Novodirect GmbH, Kehl/Rhein, Germany
Needle microlance 21G, 24G, 25G	B.Braun, Melsungen AG
96-well microtest plates	Sarstedt, Nürnbrecht, Germany
Neubauer Chamber	Hartenstein, Würzburg, Germany
15 ml, 50 ml, round bottom 50 ml conical centrifuge tubes	Sarstedt, Nürnbrecht, Germany
Parafilm M all-purpose laboratory film	Pechiney Plastic Packaging, Chicago, USA
Pasteur pipettes plain glass	VWR International, Leicestershire, UK
pH-indicator Strips pH 0 - 14 universal indicator	Merck, Darmstadt, Germany
Pipette tip 10 µl, 200 µl, 1000 µl	Sarstedt, Nürnbrecht, Germany
Safe-Lock micro test tube 2.0 ml	Eppendorf, Hamburg, Germany
SafeSeal micro tube 1.5 ml	Sarstedt, Nürnbrecht, Germany
Sterile insulin syringe 1ml	Becton, Dickinson and Company, Heidelberg, Germany
Surgical Blades, sterile	B Braun, Tuttlingen, Germany
Syringe filter 0.22 µm	Carl Roth, Karlsruhe, Germany
Syringe, 2ml, 5ml, 10ml, 20ml	B Braun, Tuttlingen, Germany
Thickwall Polycarbonate 1ml 11×34mm Tubes for Ultracentrifuge	Beckman Coulter, Brea, CA

Tissue culture flask, PE Phenolie style cap, 75cm², 175cm²	Sarstedt, Nürnbrecht, Germany
Tissue culture dish 100×20mm	Sarstedt, Nürnbrecht, Germany
Tissue culture dish 60×15mm	BD Falcon, BD Biosciences, Durham, USA
Transwell	VWR, Darmstadt, Germany
TruCount tubes	BD Biosciences, Durham, USA

3.1.3   Experimental kits and systems

Vectastain Elite ABC kit Rat IgG (Vectastain, Linearis, Wertheim-Bettingen, Germany)

3.1.4   Chemicals, reagents and customized services

Chemical/reagent	Source
(3-Aminopropyl) triethoxysilane	Sigma-Aldrich Chemie, Steinheim, Germany
[^{14}C]sphingomyelin (Bovine; [Choline-Methyl-14C],10μCi (370kBq))	Perkin Elmer, Rodgau, Germany
0.05%Typsin EDTA	Invitrogen, Darmstadt, Germany
2-mercaptoethanol	Sigma-Aldrich Chemie, Steinheim, Germany
2-methyl butane	Sigma-Aldrich Chemie, Steinheim, Germany
2-Propanol	Carl Roth, Karlsruhe, Germany
^{3}H-Thymidine	Perkin Elmer, Rodgau, Germany
Acetic acid	VWR, Darmstadt, Germany
Acetone	Hedinger, Stuttgart, Germany
Acid sphingomyelinase	Sigma-Aldrich Chemie, Steinheim, Germany
Amino-ethylcarbazol (AEC)	Sigma-Aldrich Chemie, Steinheim, Germany
Amitriptyline	Sigma, Schnelldorf, Germany
Ammonium chloride	Sigma-Aldrich Chemie, Steinheim, Germany
Antibiotic-antimycotic	Invitrogen, Darmstadt, Germany
Aquatex	Merck, Darmstadt, Germany

Brefeldin A	Sigma-Aldrich Chemie, Steinheim, Germany
Calcium chloride	Carl Roth, Karlsruhe, Germany
Casein	Merck, Darmstadt, Germany
Chloroform p.A.	Applichem, Darmstadt, Germany
Concanavalin A	Sigma-Aldrich Chemie, Steinheim, Germany
Coomassie brillant blue G 250	Carl Roth, Karlsruhe, Germany
Dimethyl sulfoxide (DMSO)	Sigma-Aldrich Chemie, Steinheim, Germany
Dimethylformamide	Sigma-Aldrich Chemie, Steinheim, Germany
Dulbecco's Modified Eagle Medium (DMEM) (High Glucose)	Invitrogen, Darmstadt, Germany
EDTA	Carl Roth, Karlsruhe, Germany
EGTA	Carl Roth, Karlsruhe, Germany
Entellan	Merck, Darmstadt, Germany
Eosin Y (aqueous)	Merck, Darmstadt, Germany
Ethanol	Sigma-Aldrich Chemie, Steinheim, Germany
Evans Blue dye	Sigma-Aldrich Chemie, Steinheim, Germany
Fetal bovine serum-South America	PAN Biotech GmbH, Aidenbach, Germany
Fibronectin	Roche, Mannheim, Germany
Formamide	Sigma-Aldrich Chemie, Steinheim, Germany
Giemsa	Merck, Darmstadt, Germany
Glucose	Merck, Darmstadt, Germany
Glutamax	Invitrogen, Darmstadt, Germany
Glutardialdehyde	Carl Roth, Karlsruhe, Germany
Glycerol	Carl Roth, Karlsruhe, Germany
H2O2 (30%)	Otto Fishar GmBH, Saarbrueken, Germany
HBSS	Sigma-Aldrich Chemie, Steinheim, Germany
HEPES	Carl Roth, Karlsruhe, Germany

HEPES	Sigma-Aldrich Chemie, Steinheim, Germany
Hydrochloric acid	Carl Roth, Karlsruhe, Germany
IGEPAL CA-630	Sigma-Aldrich Chemie, Steinheim, Germany
Incomplete Freund Adjuvant	DIFCO Laboratories, Michigan
Ionomycin	Sigma-Aldrich Chemie, Steinheim, Germany
Isopropanol	Hedinger, Stuttgart, Germany
KCL	Merck, Darmstadt, Germany
Laminin	Sigma-Aldrich Chemie, Steinheim, Germany
liquid scintillation cocktail for proteins, peptides and nucleic acids (Ready Protein$^+$)	Beckman Coulter, Krefeld, Germany
Magnesium chloride	Carl Roth, Karlsruhe, Germany
Manganese (II) chloride	Sigma-Aldrich Chemie, Steinheim, Germany
Mayers Hematoxylin	VWR, Darmstadt, Germany
Methanol	Carl Roth, Karlsruhe, Germany
Methanol	JT Baker, Griesheim, Germany
MgSO4 · 7 H_2O	Sigma-Aldrich Chemie, Steinheim, Germany
Mowiol	Sigma-Aldrich Chemie, Steinheim, Germany
Mycobacterium tuberculosis H37 Ra	BD Biosciences, Durham, USA
Myelin Oligodendrocytic peptide 35-55	Charite, Berlin, Germany
N,N-Dimethylformamide	Sigma-Aldrich Chemie, Steinheim, Germany
Paraformaldehyde (PFA)	Sigma-Aldrich Chemie, Steinheim, Germany
Pepsin Solution Digest-AU	Invitrogen, Darmstadt, Germany
Pertussis toxin	Enzo life Sciences, Lörrach, Germany
Phorbol-12-myristate-13-acetate	Sigma-Aldrich Chemie, Steinheim, Germany
PLP (139-151)	Anaspec, Fremont, USA
RPMI 1640 Medium	Invitrogen, Darmstadt, Germany

Saponin	Sigma-Aldrich Chemie, Steinheim, Germany
Sodium acetate	Sigma-Aldrich Chemie, Steinheim, Germany
Sodium azide	Sigma-Aldrich Chemie, Steinheim, Germany
Sodium bicarbonate	Merck, Darmstadt, Germany
Sodium carbonate	Sigma-Aldrich Chemie, Steinheim, Germany
Sodium chloride	Carl Roth, Karlsruhe, Germany
Sodium citrate	Sigma-Aldrich Chemie, Steinheim, Germany
Sodium hydroxide	Carl Roth, Karlsruhe, Germany
Sulfamethoxazole	Sigma, Schnelldorf, Germany
Tissue Tek	Sakura Finetech Europe, Netherlands
Trimethoprim	Sigma, Schnelldorf, Germany
Tris HCl	Merck, Darmstadt, Germany
Trypan Blue	Sigma-Aldrich Chemie, Steinheim, Germany
TWEEN 20	Carl Roth, Karlsruhe, Germany
TWEEN 20	Sigma-Aldrich Chemie, Steinheim, Germany
Xylol	Hedinger, Stuttgart, Germany
Zinc chloride	Sigma-Aldrich Chemie, Steinheim, Germany

3.1.5   Media

3.1.5.1   Antibiotics

Trimethoprim	Trimethoprim	100 mg
0.2 mg/ml	Dissolved in 500 ml sterile H_2O.	
Sulfamethoxazole	Sulfamethoxazole	500 mg
1 mg/ml	Dissolved in Trimethoprim solution above and used as drinking water in autoclaved water bottles.	

3.1.5.2 Media for cell culture

bEnd3 medium	Dulbecco's Modified Eagle Medium (DMEM; High Glucose)	445 ml
	Fetal bovine serum (56 °C water bath, 30 min inactivated)	50 ml
	Antibiotic-antimycotic (100×)	5 ml
	Filtered with 0.22 µm bottle Top Filter. Stored at 4 °C	

MAM medium	Dulbecco's Modified Eagle Medium (DMEM; High Glucose)	457 ml
	Fetal bovine serum (56 °C water bath, 30 min inactivated)	25 ml
	Antibiotic-antimycotic (100×)	5 ml
	HEPES (1M)	12.5 ml
	Filtered with 0.22µm bottle Top Filter. Stored at 4 °C	

T Cell medium	RPMI 1640Medium	435 ml
	Fetal bovine serum (56 °C water bath, 30 min inactivated)	50 ml
	Antibiotic-antimycotic (100×)	5 ml
	Glutamax	10 ml
	Filtered with 0.22 µm bottle Top Filter. Stored at 4 °C	

3.1.6 Antibodies

Antigen	Usage (Dilution)	Species	Type	Source
Mouse anti-β_1 integrin	FACS (0.25 µl/2×10^5 cells)	Rat	PE labelled monoclonal	BD Pharmingen Biosciences, Durham, USA
Mouse anti-β_7 integrin	FACS (0.25 µl/2×10^5 cells)	Rat	PE labelled monoclonal	BD Pharmingen Biosciences, Durham, USA
Mouse anti-ceramide	Cell culture	Rat	Clone S58-9	Glycobiotech, Kükels, Germany
Mouse anti-CD4	IHC (1:50)	Rat	Monoclonal	BD Pharmingen Biosciences, Durham, USA

Mouse anti-CD4	FACS (0.4 μl/2x10^5 cells)	Rat	FITC-labelled monoclonal	BD Pharmingen Biosciences, Durham, USA
Mouse anti-CD8	IHC (1:50)	Rat	Monoclonal	BD Pharmingen Biosciences, Durham, USA
Mouse anti-CD8a	FACS (1 μl/2x10^5 cells)	Rat	PerCP-labelled monoclonal	BD Pharmingen Biosciences, Durham, USA
Mouse anti-CD45	IHC (1:50)	Rat	Monoclonal	BD Pharmingen Biosciences, Durham, USA
Mouse anti-Claudin 5	IHC (5-10 μg/ml)	Mouse	Monoclonal	Invitrogen, Darmstadt, Germany
Mouse F4/80	IHC (1:100)	Rat	Monoclonal	Serotec, Düsseldorf, Germany
Mouse IgG2aκ	IHC (1:100)	Rat	Monoclonal	IQ products, Groningen, Netherlands
Mouse IgG2bκ	IHC (1:100)	Rat	Monoclonal	IQ products, Groningen, Netherlands
Mouse anti-INFγ	FACS (0.5 μl/2x10^5 cells)	Rat	PE-labelled monoclonal	BD Pharmingen Biosciences, Durham, USA
Mouse anti-GMCSF	FACS (0.5 μl/2x10^5 cells)	Rat	PE-labelled monoclonal	BD Pharmingen Biosciences, Durham, USA
Mouse anti-IL2	FACS (0.5 μl/2x10^5 cells)	Rat	PE-labelled monoclonal	BD Pharmingen Biosciences, Durham, USA
Mouse anti-IL4	FACS (0.5 μl/2x10^5 cells)	Rat	PE-labelled monoclonal	BD Pharmingen Biosciences, Durham, USA
Mouse anti-IL17	FACS (0.25 μl/2x10^5 cells)	Rat	APC-labelled monoclonal	eBioscience, Frankfurt, Germany
Zona occludins-1	IHC (2-5 μg/ml)	Rabbit	Polyclonal	Invitrogen, Darmstadt, Germany
anti-Rat IgG; Cy3 F(ab')2 Frag	IHC (1:1000)	Donkey	Cy3-labelled polyclonal	Dianova, Jackson Immunoresearch, Hamburg, Germany
anti-rabbit IgG; F(ab')2 fragment	IHC (1:100- 1:800)	Donkey	Cy3-labelled polyclonal	Dianova, Jackson Immunoresearch, Hamburg, Germany
anti-mouse IgM; F(ab')2 fragment	IHC (1:100- 1:800)	Donkey	Cy3-labelled polyclonal	Dianova, Jackson Immunoresearch, Hamburg, Germany

3.1.7 Cell lines

Designations	Growth Properties	Organism	Cell Type	Source
bEnd.3	Adherent	*Mus musculus*	Brain endothelial-polyoma middle T antigen transformed	ATCC, Wesel, Germany

3.2 Methods

3.2.1 Mice

All animal experiments were performed in compliance with the German Guide for the Care and Use of Laboratory Animals. Female SJL mice were obtained from Charles River Laboratories (Sulzfeld, Germany) at the age of 6-8 wk. Female acid sphingomyelinase-deficient (Asm -/-; protein: Asm, gene symbol: *Smpd1*) and female C57Bl6/J mice were obtained from our breeding facility. The genotype of the mice was confirmed by polymerase chain reaction (PCR) prior to experimentation.

3.2.2 Immunization, clinical scoring guide and treatment protocols

3.2.2.1 MOG emulsion preparation

The emulsion used for immunization was prepared by combining $MOG_{aa35-55}$ with 10 mg/ml CFA in a 1:1 (vol/vol) ratio in a latex-free syringe, for an end concentration of 300 μg MOG/200 μl. The solution was mixed manually with a pipette for 1 min and put on ice. The solution was then homogenized using a probe sonicator for 60 sec (2 cycles, 45% power) and again put on ice for 1 min. The sonication was repeated as previous and then frozen at -20 °C for 24 h. After 24 h, the emulsion was thawed and the 2 cycles of sonication (as described above) were repeated. The emulsion was either injected immediately or stored at -20 °C for up to one week.

For the SJL EAE model, the same procedure for the emulsion preparation was used as described above, but with $PLP_{aa139-151}$ emulsified in 4 mg/ml CFA, for an end concentration of 50 μg PLP/200 μl.

3.2.2.2   Immunization

Induction of active EAE in 6-8 wk old mice was achieved by injecting 200 µl of the MOG (Asm -/- and wt mice) or PLP (SJL mice) emulsion, as prepared above, subcutaneously into the axillary and inguinal lymph node regions (50 µl/lymph node region). On days 0 and 2, 300 ng pertussis toxin dissolved in PBS up to a volume of 200 µl was injected intra-peritoneally (i.p.).

3.2.2.3   Clinical scoring guide

Clinical disease was checked daily and scored as previously described (Engelhardt et al., 1997):

- 0.5: Limp tail
- 1: Hind leg weakness
- 2: Hind leg paraparesis.
- 3: Hind leg paraplegia and incontinence
- 4: Fore limb and hind leg paresis.
- 5: Death

3.2.2.4   Amitriptyline treatment protocol

Beginning on days 0 or 10 post-immunization (p.i.) and continuing for the duration of the experiment, 25 mg/kg amitriptyline dissolved in sterile distilled water was injected i.p. every 12 h. The bi-daily (b.i.d.) dosing schedule was chosen to maintain a constant plasma level of amitriptyline. Sterile distilled water was used as the control.

3.2.2.5   Bone marrow transplantation

Asm -/- recipient mice (6 wk old) were exposed to 10 Gy whole-body irradiation given as split doses of 2×5 Gy with a 4 h interval using a linear accelerator (γ-source). Donor bone marrow cells (1×10^7 per mouse) derived from wt mice were then injected, via the tail vein, into each recipient. Transplanted mice were housed in autoclaved cages and treated with antibiotics in drinking water (0.2 mg/ml trimethoprim and 1 mg/ml sulfamethoxazole) for 3 wk after irradiation.

3.2.3 Tissue collection

Mice were anesthetized with isoflurane and perfused through the left heart ventricle with 4% paraformaldeyde; spinal cord was harvested, and either dehydrated for paraffin embedding or placed in Tissue Tek and snap-frozen in isopentane with liquid nitrogen at -80 °C for cryo-sectioning. The frozen tissue was cut serially in 6 μm sections on a cryostat microtome and fixed with acetone at -20 °C. Paraffin embedded tissue was serially cut at 0.5-6 μm on a microtome. Both frozen and paraffin-embedded tissue sections were placed on silanized slides to ensure adherence during staining protocols. The protocol for slide silanization was as follows:

- 3 dips in Acetone
- 1 min in 5% (v/v) Silane in Acetone
- 3 dips in Acetone
- 3 dips in dH$_2$0
- dry 24 h in 37 °C incubator

3.2.4 Assessment of vascular leakage

Evans Blue dye (EBD; 12.5 mg/kg) was administered intravenously (i.v.) in Asm -/- and wt mice at the peak of disease and allowed to circulate for 4 h before the mice were put to death. These mice were perfused through the left ventricle with 10 ml PBS to remove intravascular dye, then the spinal cord was either taken for quantitative analysis using fluorescence detection or fixed overnight in 4% PFA then snap frozen in Tissue Tek. 30 μm sections were taken on the cryostat microtome, air-dried and acetone fixed for 2 min. The sections were dipped in xylol and cover-slipped with Entellan.

3.2.5 Fluorescent detection of Evans Blue dye

Quantitative evaluation of EBD was performed on the spinal cord of both Asm -/- and wt immunized mice at the peak of disease. Spinal cord samples were weighed (SCW), homogenized in 250 μl formamide and incubated for 24 h at 37°C. The samples were then centrifuged at 5000 x g for 30 min. The absorption (A) of EBD in the spinal cord supernatant was measured at 620 nm. The concentration of EBD in the spinal cord was then determined against a standard curve and calculated with the equation: ngEBD = 22.411(A$_{620}$) - 0.4165. The degree of vascular leak in each spinal cord is presented as the amount of EBD/weight of

spinal cord (ngEBD/mg). Experiments were performed in collaboration with the group of Dr. E. Gulbins.

3.2.6 Histology

3.2.6.1 Basic stains

Hematoxylin and Eosin staining was performed on spinal cord of wt and Asm -/- mice. The protocol used was performed exactly as described in the Mayer's Hematoxylin protocol from Sigma:

1. Deparaffinize to water or fix and hydrate frozen sections.
2. Stain in Mayer's Hematoxylin Solution for 15 min
3. Rinse in warm running tap water for 15 min
4. Place in distilled water for 30 sec
5. Place in Eosin Y Solution (aqueous) counterstain for 30–60 sec
6. Dehydrate and clear through 2 changes each of 95% Reagent Alcohol, absolute Reagent Alcohol, and xylene (2 min each)
7. Mount with Entellan.

3.2.6.2 Immunohistochemistry

Immunohistochemistry for CD45, CD4, CD8 and F4/80 was performed on frozen serial sections using a three-step immunoperoxidase technique in a humidified chamber exactly as described previously by Walter *et al*. (Walter et al., 2002):

1. Thaw tissue for 10 min in a dehydration chamber
2. Fix in acetone -20 °C for 10 min
3. Let dry in fume hood
4. Wash in 1x PBS for 5 min
5. Block in 0,2% Casein for 45 min
6. In humidified chamber, put 100 µl primary antibody (in PBS 0,1% Tween 20), or Isotype control (in PBS 0,1% Tween) on tissue encircled with a DAKO pen for 1 h at RT
7. Wash in PBS 0,1% Tween 20 for 5 min
8. In humidified chamber, put 100 µl AK Goat-anti-rat Biotin from Vectastain kit (use 5µl in 1 mL of PBS for dilution) for 30 min
9. Wash in PBS 0,1% Tween 20 for 5 min

10. In humidified chamber, put 100 µl Strep-HRP from Vectastain kit for 30 min

11. Wash in PBS 0,1% Tween for 5 min

12. Put 100 µl AEC dye solution (100 µl AEC dissolved in dimethylformamide (8 mg/ml)/1,4 mL AEC buffer (7,9 mL Na Acetate (0,1 M) + 2,1 mL Acetic acid (0,1 M))/1,5 µl H2O2) on tissue until red (approximately 3-10 min)

13. When tissue is ready, pour off AEC into waste container and stop reaction with PBS

14. Counterstain with Mayer's Hematoxylin, approximately 1 min, until tissue is purple

15. Rinse with dH$_2$0 x 3 and tap water x 3 until water is clear and let sit approximately 20 min

16. Coverslip with Aquatex

Immunohistochemistry for tight junctions, including Zona occludins-1 (ZO-1) and claudin-5, was performed on paraffin sections of spinal cord. Paraffin sections were dewaxed, washed in H$_2$0, blocked in H/S supplemented with 5% FCS, washed in PBS, incubated with Pepsin for 12 min, washed in PBS and incubated with anti-ZO-1 antibodies or anti-claudin-5 antibodies for 45 min in H/S + 5% FCS. Samples were washed 3-times in PBS supplemented with 0.5% Tween 20 and once in PBS, incubated for 45 min with Cy3-conjugated antibodies diluted 1:1000 in H/S + 5% FCS. Samples were washed again 3-times in PBS/0.05% Tween 20 and once in PBS, embedded in Mowiol and analysed by confocal microscopy. Experiments were performed in collaboration with the group of Dr. E. Gulbins.

3.2.7 bEnd.3 cell culture

The brain endothelial cell line (bEnd.3) used for the experiments were cultured and sub-cultured as per the recommendation from ATCC. The cells were grown in bEnd.3 complete growth medium in an incubator at 37 °C and 5% carbon dioxide (CO_2). When the flasks were full and ready to subculture, culture medium was removed and discarded. The cell layer was rinsed with 0.25% (w/v) Trypsin-0.03% (w/v) EDTA solution to remove all traces of serum (which contains trypsin inhibitor). Then 5 ml of Trypsin-EDTA solution was added to each flask and the cells observed under an inverted microscope until the cell layer just began to detach. 5 ml of complete growth medium was then added and the cells aspirated by gently pipetting. Cell suspensions were collected in 50 ml falcon tubes and centrifuged for 8 min

(1200 rpm). The supernatant was removed and the cells resuspended in new growth medium to create a subcultivation ratio of 1:2 to 1:4 (5 ml/flask). The medium was renewed every 2-3 days and subcultivated every 7 days. To freeze cells for preservation, cells were collected from 2-3 flasks and suspended in freezing medium (complete growth medium, 95%; DMSO, 5%) in a cryotube. Cryotubes were placed in a "Mr Frosty" freezing container at -80 °C for 24-48 h, then stored permanently in liquid nitrogen vapor.

3.2.8 *In vitro* adhesion assay

Determination of adherence of lymphocytes to an endothelial mono-layer was performed as described by Reiss *et al.* (Reiss et al., 1998). Briefly, 16 well chamber slides were coated with 50 μg/ml fibronectin and then plated with bEnd.3 cells ($2x10^4$/ well) for 2 days prior to the experiment. T lymphocytes were obtained by homogenizing mouse axillary, inguinal and mesenteric lymph nodes in a HBSS/10% FCS/1% HEPES solution and strained through a 70μm cell filter. Cell suspensions were centrifuged (1200 rpm, 8 min, 4 °C) and re-suspended in MAM medium. T cells ($3x10^5$ cells/well in MAM medium) were co-incubated with the endothelial cells for 40 min at 4 °C on a rocking shaker. Following co-incubation, non-adherent T cells were washed off with PBS and the slides fixed in 2.5% glutardialdehyde for 2 h. Assays were counted with a light microscope following the fixation period. The following substances were tested: 10 μM amitriptyline (30 min pre-incubation at RT), 1 U/ml acid sphingomyelinase (30 min pre-incubation at RT) and 1 mmol Mn2+ (co-incubation with bEnd.3 cells) All experiments were done in the presence of 10 μM ZnCl and performed in duplicate.
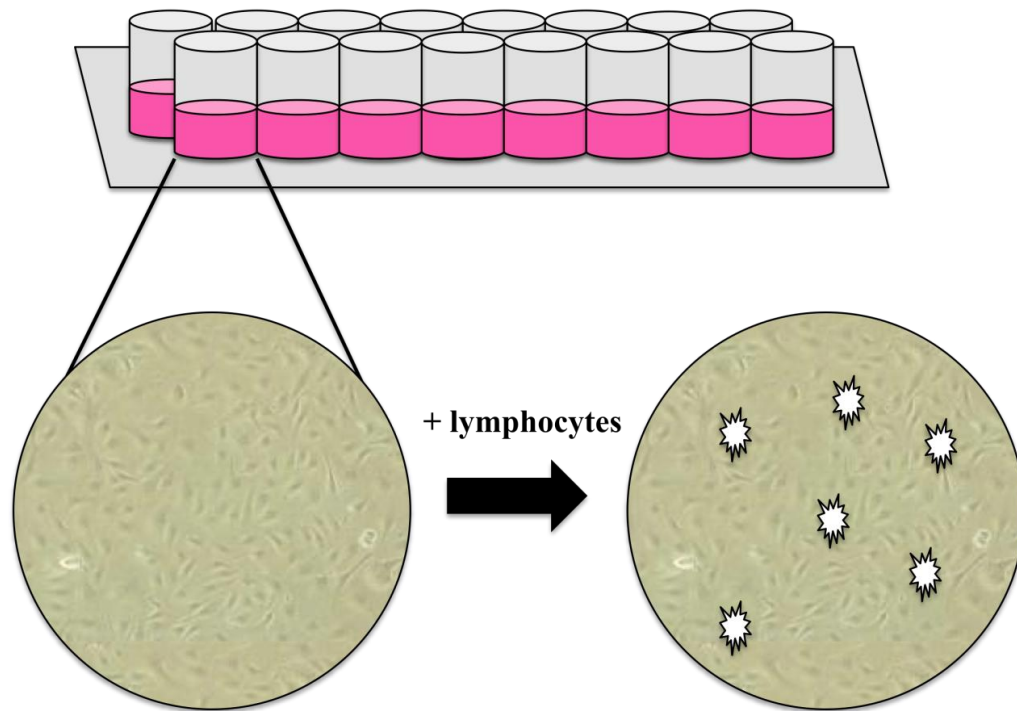
bEnd.3 brain endothelial monolayer

Figure 3.1 Adhesion assay method diagram.

3.2.9 *In vitro* transmigration assay

In-vitro analysis of T cell transmigration through an endothelial mono-layer was performed as described by Rohnelt *et al*. (Rohnelt et al., 1997). Briefly, the filter from a Transwell double chamber system was coated with 50 µg/ml laminin and following a 30 min incubation time at RT, bEnd.3 cells ($5x10^4$/well) were plated and incubated (37 ºC, 10% CO_2) for 2 days. At the time of the assay, 600 µl MAM medium was added to the lower compartment and 100 µl containing $1x10^6$ lymphocytes was aliquoted to the upper compartment for 4h incubation at 37 ºC. Following the co-incubation, the medium from the lower compartment was removed and transferred to TruCount tubes to be analysed by flow cytometry to determine the number of migrated cells. The filters were washed with PBS then fixed in a formaldehyde-saturated chamber overnight and stained with Giemsa to verify a confluent bEnd.3 layer. All experiments were done in the presence of 10 µM ZnCl and performed in duplicate.

3.2.10 Proliferation assay

On day 10 p.i., T cells were isolated and cultured in a 96 well plate (2×10^5/well) in re-stimulation medium (T cell medium/0.1% 2-mercaptoethanol), 2.5 µg/ml Concanavalin A or MOG antigen. The cells were cultured for 48 h at 37 ℃. Following incubation, cells were pulsed with ^{3}H-Thymidine (1 µCi/well) and incubated for a further 16 h at 37 ℃. Cells were then transferred onto a glass fibre filter for measurement of tritiated thymidine by a liquid scintillation counter. Means and SEM were calculated from duplicate or triplicate wells.

3.2.11 Surface and intracellular expression of adhesion molecules and cytokines

For extracellular antibody staining, 2×10^5 T cells (day 14 p.i.) were washed and re-suspended in FACS buffer (1x PBS/ 4% FCS/ 0.4% sodium azide). Anti-β-1 integrin or anti-β-7 integrin was then added along with anti-CD4 and anti-CD8a to determine the number of positive cells within the T cell population from the sample. Cell surface staining was performed with the appropriate combination of antibodies conjugated to fluorescein isothiocyanate, allophycocyanin, phycoerythrin, and peridinin-chlorophyll protein complex. The antibody/cell suspension was incubated at 4 °C for 40 min then washed and analyzed by flow cytometry with FACScanto using the FACS Diva Software.

For cytokine staining, 2×10^5 cells were incubated at 37 °C for 4 h in T cell medium with 500 ng/ml Ionomycin, 50 ng/ml Phorbol-12-myristate-13-acetate (PMA) and 10 µg/ml Brefeldin for stimulation. Following the incubation period, the cells were permeabilized with 0.1% Saponin for the intracellular cytokine staining. The cells were then incubated at RT for 30 min with anti-interleukin-2 (IL-2), anti-IL-4, anti-IL-17, anti-interferon-γ (IFNγ) or anti-granulocyte macrophage colony-stimulating factor (GMCSF) along with anti-CD4 and anti-CD8a. The cells were then washed and analyzed as above.

3.2.12 Ceramide clustering

To determine the clustering of β1-integrin with ceramide rafts on the cell surface of T cells, we used confocal microscopy of T cells co-incubated with a bEnd.3 monolayer. Two days before the assay, 1×10^5 bEnd.3 cells were plated on glass coverslips in a 24-well plate. On day 14 p.i., T cells were harvested from wt and Asm -/- mice as described above, and 5×10^5 T cells were co-incubated with the bEnd.3 monolayer for 5, 10, 15, or 20 min. The cells were

removed, pelleted and fixed in 4% PFA for 15-min. After fixation, the slides were washed in PBS and blocked in HEPES/Saline (H/S; 132 mM NaCl, 20 mM HEPES [pH 7.4], 5 mM KCl, 1 mM $CaCl_2$, 0.7 mM $MgCl_2$, 0.8 mM $MgSO_4$) supplemented with 5% FCS and 0.05% Tween 20 for 10 min. Anti-ceramide antibody clone S58-9 was diluted 1:100 in H/S + 1% FCS and cells were incubated for 45 min with the anti-ceramide antibody. Cells were then washed 3 times in PBS, incubated for 45 min with Cy3-coupled donkey anti-rabbit IgG or anti-mouse IgM F(ab)$_2$ fragments, washed again three times in PBS, resuspended in 5 μl of PBS, pipetted onto a glass slide and embedded in Mowiol. Immunofluorescence was measured with the Leica TCS SL software program, version 2.61. Experiments were performed in collaboration with the group of Dr. E. Gulbins.

3.2.13 Acid sphingomyelinase activity

In order to determine the successful transplantation of wt bone marrow in Asm -/- mice, at the time of sacrifice, spleen was harvested from each animal and homogenized to a single cell suspension. Spleen cells were pelleted and lysed in 250 mM sodium acetate (pH 5.0), 1% NP40, and 1.3 mM EDTA for 5 min. Lysates were diluted to 250 mM sodium acetate (pH 5.0), 0.1% NP40, and 1.3 mM EDTA and incubated with 50 nCi per sample [^{14}C]sphingomyelin for 30 min at 37 °C. The sphingomyelin was dried prior to the assay, resuspended in 250 mM sodium acetate (pH 5.0), 0.1% NP40, and 1.3 mM EDTA and bath-sonicated for 10 min. The reaction was stopped by the addition of 800 μL chloroform/methanol (2:1, v/v), phases were separated by centrifugation and radioactivity of the aqueous phase was measured by using liquid scintillation counting to determine the release of [^{14}C]phosphorylcholine from [^{14}C]sphingomyelin as a measure of Asm activity. Experiments were performed in collaboration with the group of Dr. E. Gulbins.

3.2.14 Statistics

Data in figures are presented as mean + SEM. One-way ANOVA followed by Tukey's HSD post hoc test was used for multiple comparisons. Two-independent samples t test was used to compare means for two groups. All statistical analysis was performed on GraphPad Prism for Windows (GraphPad software, La Jolla, CA). Statistical significance was set at $p < 0.05$.

4 Results

4.1 Asm deficiency protects against EAE development

To determine whether Asm plays a role in the development of EAE, we immunized Asm -/- and C57BL/6 wt mice with MOG_{35-55} in complete Freund's adjuvant (CFA) followed by two injections of pertussis toxin. The wt animals exhibited clinical symptoms from day 10 p.i., starting with limp tail and hind-leg paresis. The disease peaked at day 19 with a mean clinical score of 2 and maximum clinical score of 5 (death). In contrast, all Asm-deficient animals exhibited no or very mild clinical symptoms, with a limp tail score of 0.5 at maximum even after prolonged observation (up to day 30 p.i.). Daily clinical scoring of the percentage of symptomatic mice showed a significant difference between wt and Asm -/- groups starting from day 14 and continuing to day 22 ($p \leq 0.05$, t-test), after which point all the mice from the wt group had been sacrificed for ethical reasons (Fig. 4.1).
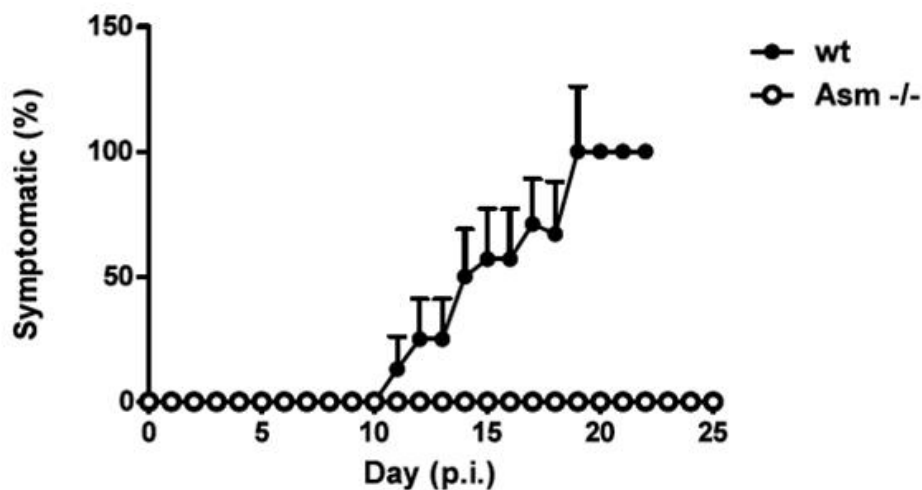

Figure 4.1 Genetic Asm deficiency prevents active EAE over a 25-day period. Mice were immunized with MOG_{35-55} in complete Freund's adjuvant (CFA). Animals were evaluated daily for clinical symptoms. The data show that deficiency of Asm afforded protection against developing symptoms of EAE. There was a significant difference in % symptomatic mice from day 14-22 ($p \leq 0.05$, t-test). Shown are means +SEM of 9 wt and 7 Asm -/- mice.

Further, wt mice developed an EAE-typical weight loss and only regained 0.63 +/- 0.72 g (mean +/- SEM) at day 25; Asm-deficient mice were resistant to weight loss and gained 2.56 +/- 0.62 g (mean +/- SEM) by day 25 (Fig. 4.2).
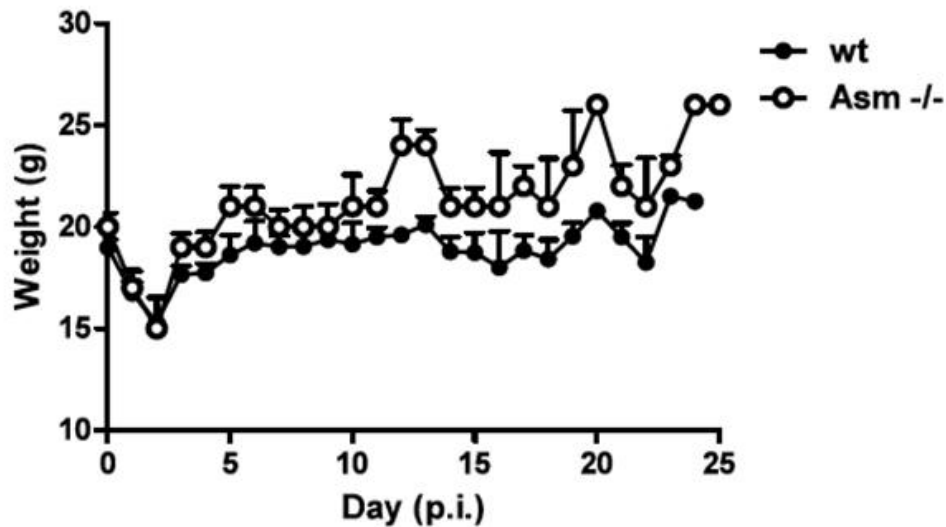

Figure 4.2 Genetic Asm deficiency prevents weight-loss associated with active EAE induction. Mice were immunized and weighed daily. The data show that deficiency of Asm afforded protection against developing weight-loss associated with EAE. The starting weight of wild-type mice and Asm-/- mice were not significantly different ($p \geq 0.05$, t-test), while the final weight of the Asm -/- mice was significantly higher ($p \leq 0.05$, t-test). Shown are means + SEM of 9 wt and 7 Asm -/- mice.

Further analysis of a large number of immunized wt and Asm-deficient mice that were used in experiments described below to investigate lymphocyte functions and histology changes in the central nervous system, confirmed the results of these kinetic studies and showed that 93% of the wt mice exhibited symptoms up to grade 5, whereas 89% of the Asm-deficient animals were unaffected and 11% developed only mild clinical symptoms (Fig. 4.3). The average clinical score of the wt mice was 1.6 +/- 0.15 (mean +/- SEM).
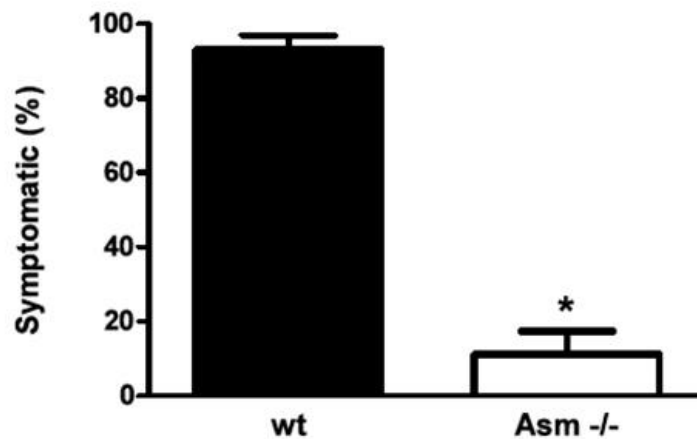
Figure 4.3 Genetic Asm deficiency prevents active EAE. Mice were immunized for various experiments and evaluated for clinical symptoms at the time of sacrifice. The data show that deficiency of Asm afforded protection against developing symptoms of EAE. Shown are means + SEM of 59 wt and 28 Asm -/- mice (*$p \leq 0.05$, t-test).

The clinical resistance of Asm-deficient mice to EAE was associated with the absence of inflammatory infiltration in spinal cord, as determined by CD45 staining (Fig. 4.4), whereas wt mice exhibited a prominent infiltration with CD45, CD4, CD8 and F4/80 positive leukocytes in the spinal cord (Fig. 4.4 and 4.5).
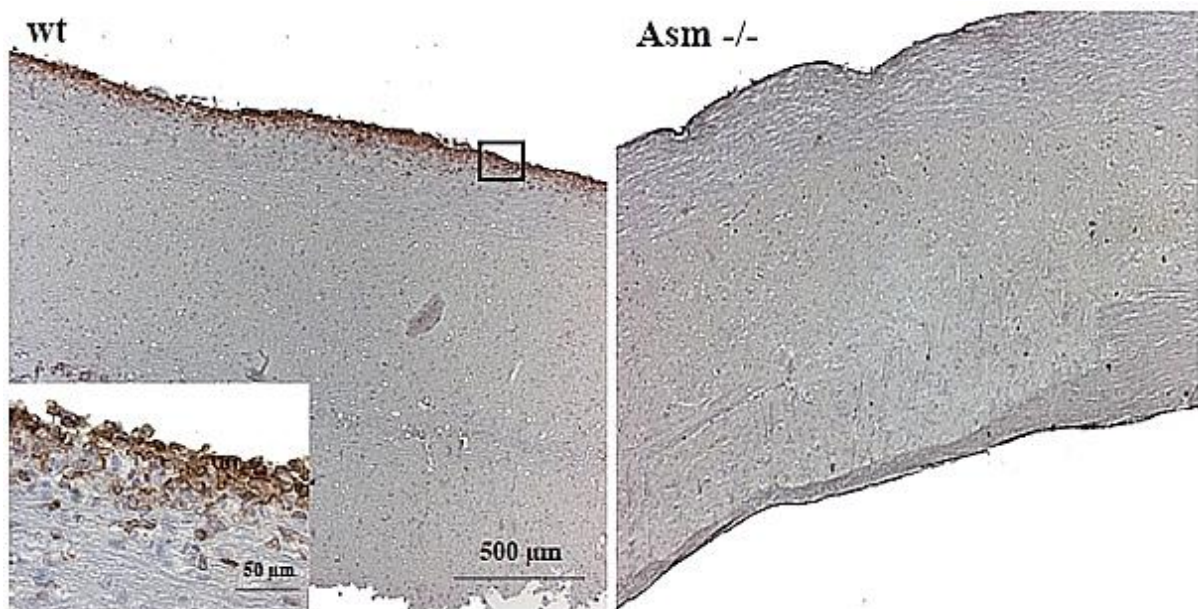

Figure 4.4 Genetic Asm deficiency protects against leukocytic infiltration into central nervous system tissue. Asm -/- and wt mouse spinal cord frozen sections (6 μm) were stained with CD45 to assess infiltration of leukocytes. The left panel (wt) reveals characteristic leukocytic infiltration in a wt mouse spinal cord sacrificed at peak of disease. The right panel (Asm -/-) shows the lack of cellular infiltration in the spinal cord of an Asm deficient mouse taken at the same time point. These images are representative of all mice in the study.
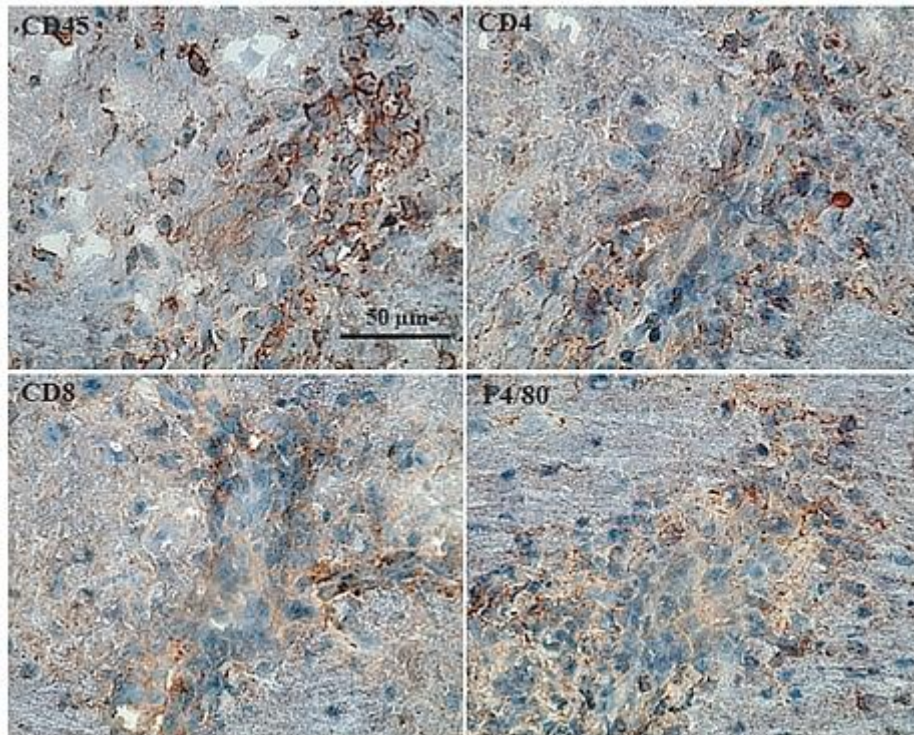
Figure 4.5 Characteristic inflammatory infiltrates composed of predominantly T cells. Immunohistochemical staining of frozen sections (6 μm) revealed characteristic cellular infiltrates in the spinal cord of wt mice. The majority of the cells stained positively for CD45 (a leukocyte marker) with CD4 staining as the major subset of T cells. There was also positive staining of cells for CD8 and F4/80 (a macrophage marker). These results are typical for EAE and are representative of multiple samples.

4.2 Asm deficiency preserves BBB integrity and tight junctions in EAE

BBB breakdown is one of the main pathophysiological features resulting in inflammatory infiltration with clinical symptoms in EAE. In order to elucidate the influence of Asm on the BBB integrity, we injected Evans Blue into MOG immunized wt and Asm deficient mice. We observed a massive Evans Blue intraparenchymal leakage in wt but not in Asm-deficient mice (Fig. 4.6). Through quantitative analysis, we were also able to show a significantly decreased leakage of Evans Blue dye in Asm -/- mouse spinal cord (Fig. 4.7).
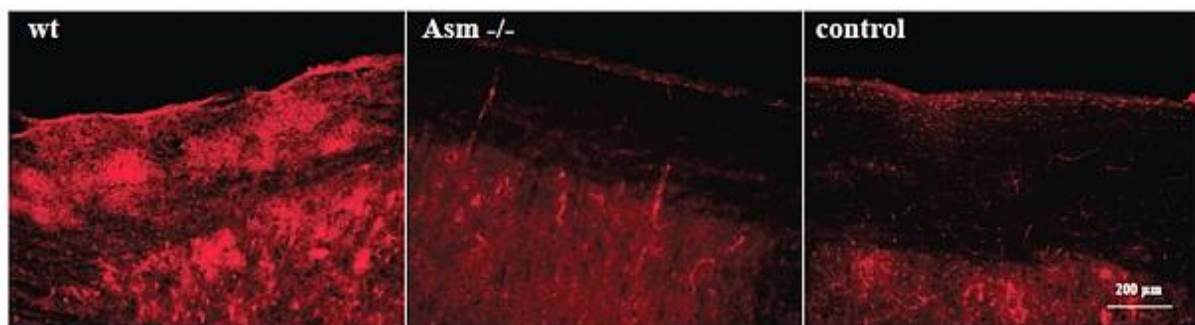

Figure 4.6 BBB integrity remains intact in Asm deficient mice. Evans Blue dye (12.5 mg/kg) was injected i.v. at the peak of disease. Spinal cord frozen sections (30 µm) were analyzed under fluorescence microscopy and revealed significant leakage of Evans Blue dye in wt mice with no leakage in Asm -/- mice. Non-immunized control mouse shown for comparison.
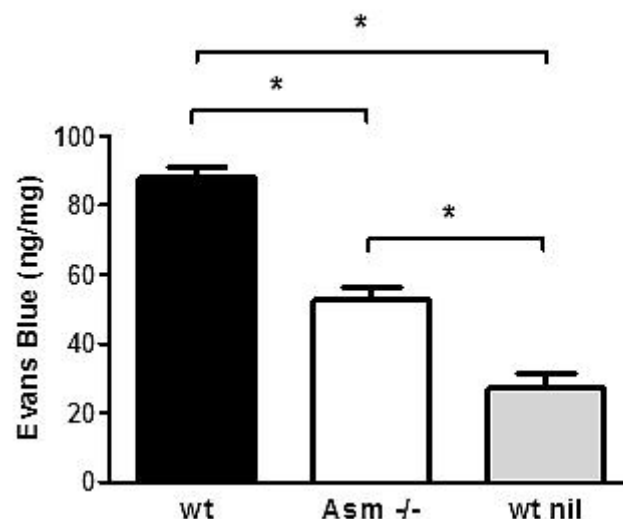

Figure 4.7 BBB integrity is significantly more compromised in wt compared to Asm deficient mouse spinal cord. Evans Blue dye was injected i.v. at peak of disease. Spinal cord was isolated, homogenized and assessed for quantitative analysis of intraparenchymal Evans Blue dye by spectrophotometry. Non-immunized control mice (n=3) are shown for comparison. The amount of Evans Blue dye in Asm -/- spinal cord was significantly less than the amount quantified in wt mouse spinal cord, and wt nil control was significantly less than either of the experimental groups (*$p \leq 0.05$, one-way ANOVA). Values are shown as mean + SEM from 5 wt mice and 5 Asm -/- mice.

The notion that Asm deficiency protects from disruption of the BBB during EAE is also supported by the finding that tight junctions remain intact in Asm-deficient EAE immunized mice but are disrupted in EAE immunized wt mice, as indicated by the degradation of ZO-1 and Claudin-5 (Fig. 4.8).
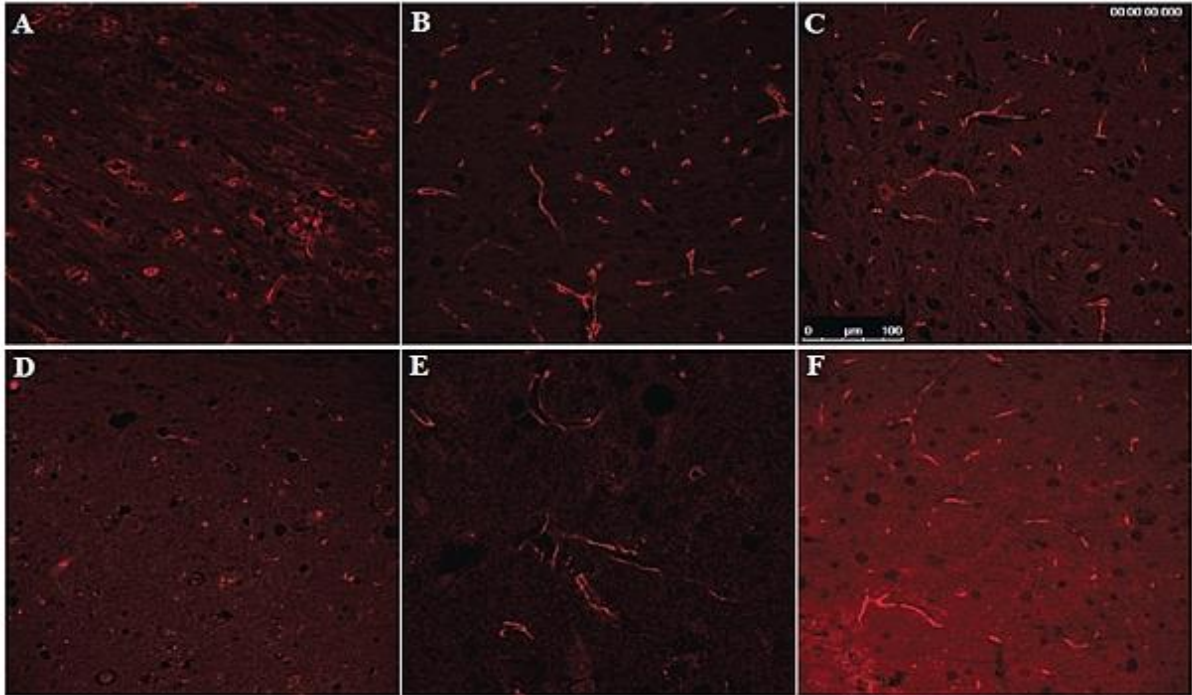

Figure 4.8 Tight junction integrity is maintained in Asm-deficient mice. Immunofluorescence staining for claudin-5 (Panel A-C) and ZO-1 (Panel D-F) revealed tight junction breakdown in wt (A & D) spinal cord, while Asm -/- (C & F) mice had intact tight junctions. Non-immunized wt control (B & E) is shown for comparison.

4.3   Asm in lymphocytes is sufficient to induce EAE

To further differentiate the importance of endothelial versus lymphocytic Asm in EAE development, we irradiated Asm-deficient mice with 10 Gy and transplanted them with bone marrow from syngenic wt mice. Control studies measuring Asm activity in the spleen confirmed successful bone marrow transplantation. Immunization of these mice with MOG_{35-55} and pertussis toxin resulted in a severe EAE up to grade 2 indicating that Asm-expression in lymphocytes is sufficient to induce EAE (Fig. 4.9). The clinical data was corroborated with histology, and showed leukocyte infiltration in Asm -/- mice transplanted with wt bone marrow cells (Fig. 4.10).
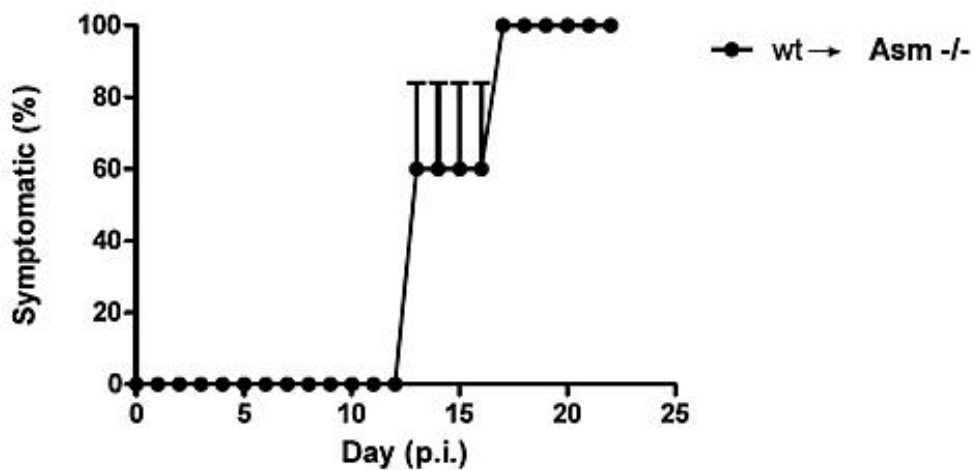
Figure 4.9 Bone marrow transplantation of wt cells into Asm deficient mice confers susceptibility to EAE disease. Asm -/- mice were irradiated with 10 Gy and transplanted with wt bone marrow cells (1×10^7 per mouse). The recipient mice were immunized with MOG following bone marrow reconstruction and scored daily. The Asm -/- recipient mice (wt donor cells) became as clinically ill as wt control, with no significant difference in peak clinical score ($p \geq 0.05$, t-test). Values presented are mean + SEM for 5 Asm -/- recipient mice.

Figure 4.10 Bone marrow transplantation of wt cells into Asm deficient mice abolishes protection against leukocytic infiltration. Immunohistochemical analysis of spinal cord with CD45 corroborates the clinical findings after bone marrow transplantation and reveals inflammatory infiltrates in Asm -/- recipient mice that have been reconstructed with wt bone marrow. Images are representative of 5 Asm -/- recipient mice.
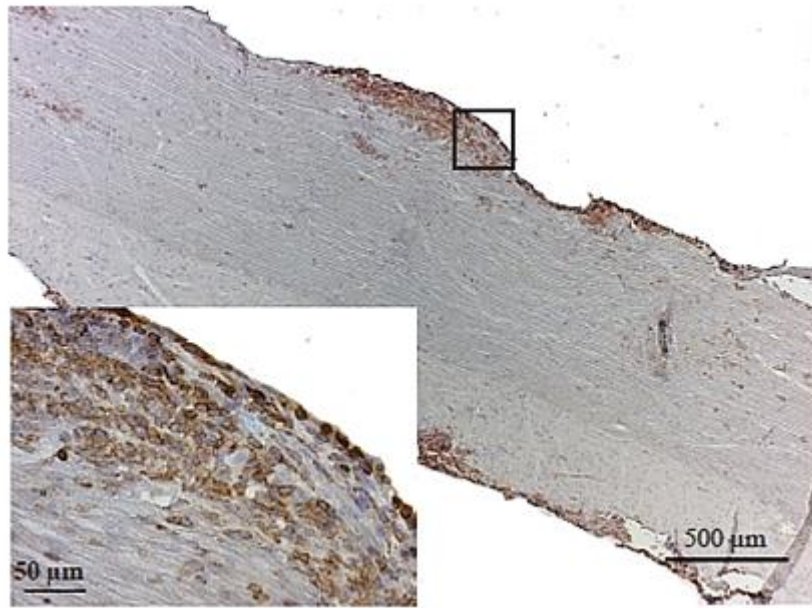
4.4 Asm does not control lymphocyte proliferation, integrin or cytokine expression

To identify molecular mechanisms that prevent EAE in Asm-deficient mice, we tested whether Asm deficiency affects antigen-specific proliferation, which is a main requirement for induction of the autoimmune process during EAE. To this end we examined the proliferation capacity of Asm-deficient lymphocytes derived from EAE-immunized mice by using a ^{3}H-thymidine assay. We observed no difference in MOG-induced proliferation between Asm-deficient and wt cells (Fig. 4.11).
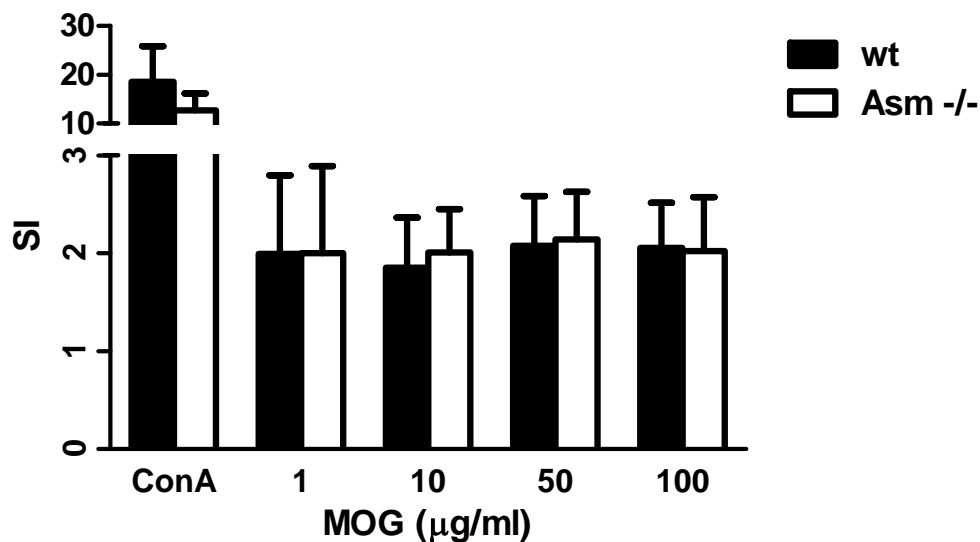
Figure 4.11 Asm deficiency does not affect proliferation of MOG stimulated lymphocytes. Using a ^{3}H-thymidine proliferation assay, we were able to show that there was no significant difference in lymphocyte proliferation between wt and Asm -/- cells (p ≥ 0.05, t-test) at various concentrations of MOG peptide and Concanavalin A control. Values presented as mean +/- SEM for 7 wt and 7 Asm -/- mice from 7 independent experiments. SI = counts per minute of stimulated lymphocytes/ counts per minute of unstimulated lymphocytes.

Furthermore, we detected neither a difference in the expression levels of beta integrins on lymphocytes (Fig. 4.12) nor a difference in the production of inflammatory cytokines, e.g., IL-2, IL-4, IL-17, IFNγ, or GM-CSF, (Fig. 4.13) by spleen- or lymph node–derived CD4^{+} or CD8^{+} T cells from Asm-deficient or wt mice after cell stimulation. Collectively, this data indicates that Asm does not mediate early T cell activation in EAE.
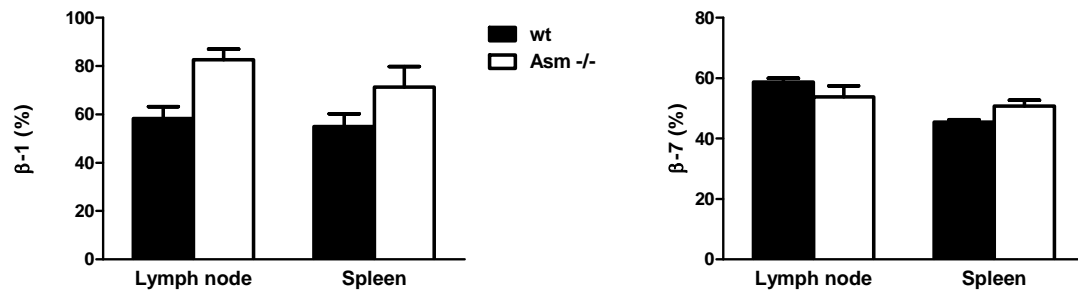
Figure 4.12 Asm deficiency does not affect expression of β-1 or β-7 integrin. Lymphocytes from wt and Asm -/- mice were isolated at day 14 p.i. and analyzed for β-1 and β-7 integrin cell surface expression using flow cytometry. The expression of these integrins was not significantly different between wt and Asm -/- cells derived from lymph node or spleen. Values presented as mean + SEM (p≥ 0.05, t-test) for 6 wt and 6 Asm -/- mice.

Figure 4.13 Asm deficiency does not affect expression of cytokines. Lymphocytes from wt and Asm -/- mice were isolated at day 14 p.i. and analyzed for expression of IL-2, IL-4, IL-17, GMCSF and IFNγ using flow cytometry. The expression of these cytokines was not significantly different between wt and Asm -/- cells derived from lymph node or spleen. Values presented as mean + SEM (p≥ 0.05, t-test) for 6 wt and 6 Asm -/- mice.
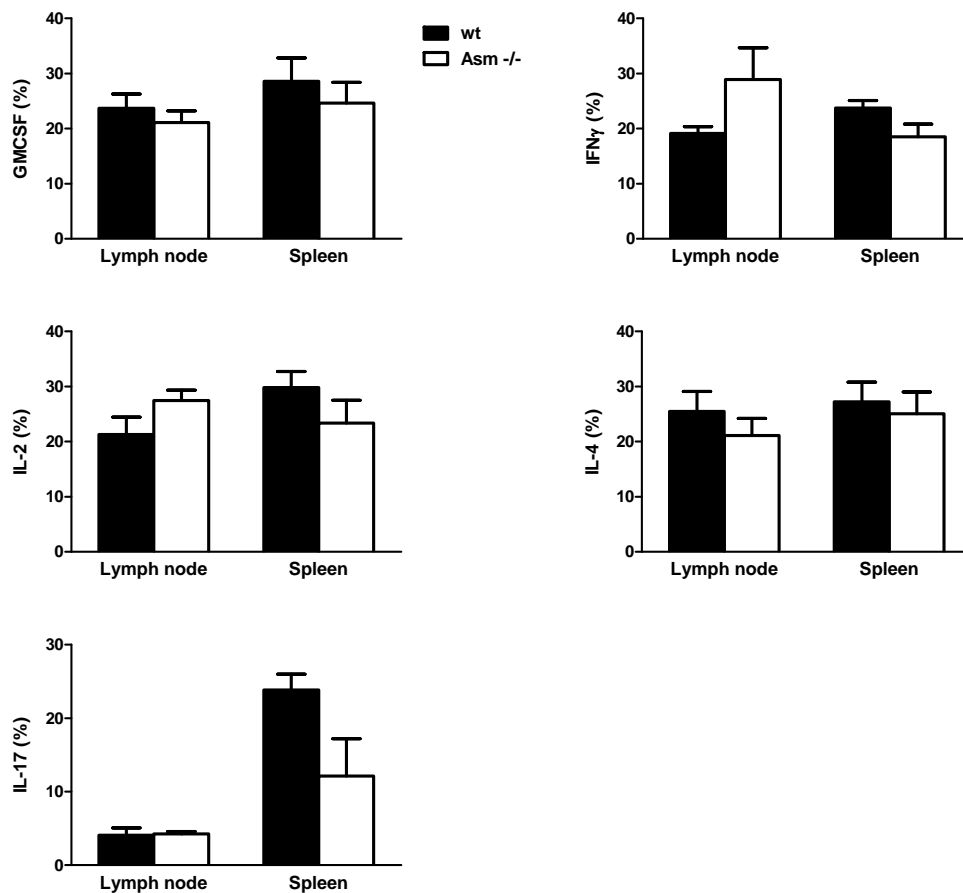
4.5   Asm is required for β-1 integrin-mediated lymphocyte-endothelial cell adhesion

4.5.1   Adhesion

Endothelial adhesion and subsequent migration of lymphocytes through the BBB is an important pathophysiological step in the development of EAE. To determine the adhesion and transmigration capability of freshly isolated lymphocytes from wt and Asm-deficient EAE mice, we performed *in vitro* adhesion and transmigration assays using the bEnd.3 endothelial cell line to model the BBB.

Adhesion to bEnd.3 cells was 60% lower in lymphocytes from Asm-deficient EAE-immunized mice than in wt EAE lymphocytes (Fig. 4.14). Restoration of Asm in Asm-deficient lymphocytes re-established adhesion capability to wt levels.
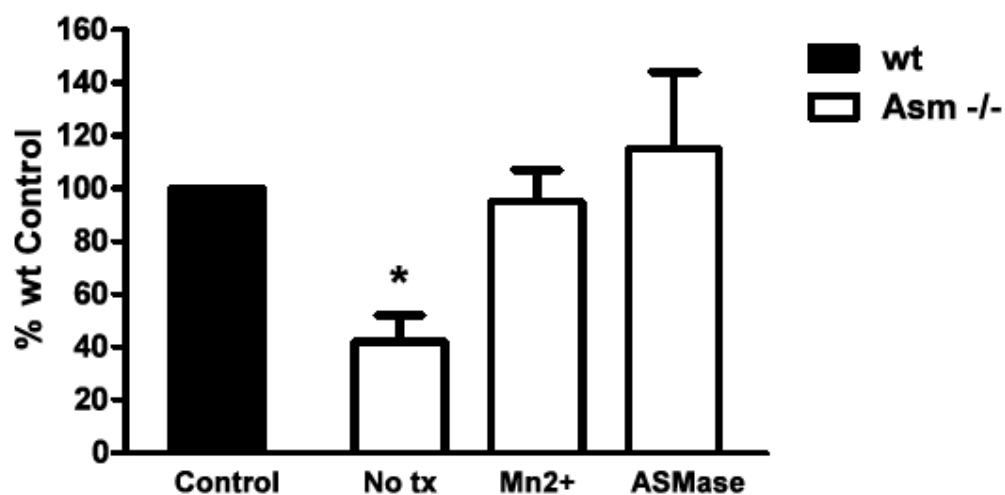
Figure 4.14 Asm deficiency reduces lymphocyte adhesion to endothelial cells. In vitro adhesion assays showed a significant reduction in the adhesion of Asm-deficient lymphocytes to bEnd.3 cells. Restoration of the Asm enzyme or treatment with the integrin activator, Mn^{2+}, re-enabled lymphocyte adherence. Shown are means + SEM of wt control (n=10), Asm -/- No tx (n=10), Asm -/- treated with Mn^{2+} (n=10), and Asm -/- treated with ASMase (n=9). *p $\leq$ 0.05, t-test.

During EAE, firm adhesion of lymphocytes to the endothelium is mainly dependent on β-1 integrins. Likewise, β-1 integrin expression in lymphocytes is absolutely required for EAE induction (Bauer et al., 2009). To further prove that Asm-deficiency affects integrin activation, we tested whether Mn^{2+}, which directly activates integrins, restores adhesion of Asm-deficient lymphocytes to bEnd.3 cells (Fig. 4.14). The data shows that addition of Mn^{2+} re-enabled Asm-deficient lymphocytes to adhere to bEnd.3 cells.

4.5.2 β-1 integrin clustering in ceramide rafts

It has been previously shown that ASM-released ceramide forms large membrane platforms which serve to cluster receptor molecules (Gulbins and Li, 2006). Clustering of integrins has been shown to be a prerequisite for the proper functioning of these molecules (Grassme et al., 2001b). To test whether ASM and ceramide mediate the clustering of β-1 integrin, the most prominent adhesion molecule at the BBB during EAE (Bauer at al., 2009) in EAE lymphocytes, we prepared T cells from EAE-immunized wt and Asm -/- mice and challenged them with bEnd.3 cells. Through our collaboration with the group of Dr. E. Gulbins, we observed rapid clustering of β-1 integrin in ceramide-enriched membrane platforms after EAE-lymphocytes contacted bEnd.3 cells (Fig. 4.15).
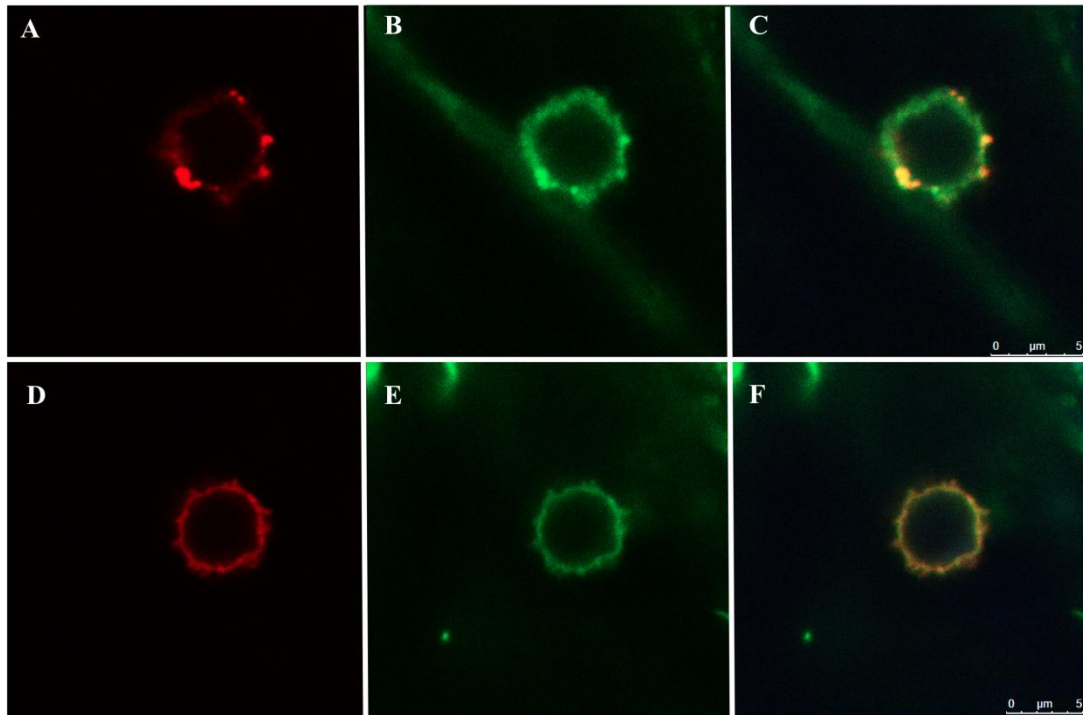
Figure 4.15 Asm induces β-1 integrin clustering in ceramide-enriched membrane platforms. Confocal microscopy analysis of experimental autoimmune encephalomyelitis-derived lymphocytes from Asm deficient or wt mice after challenge with bEnd.3 cells showed clustering of β-1 integrin in ceramide-enriched membrane platforms only in wt cells (C), whereas the receptor remained uniformly distributed in the plasma membrane of Asm-deficient lymphocytes (F). Panel A-C is a wt lymphocyte; Panel D-F is an Asm -/- lymphocyte; Panel A & D are ceramide staining; Panel B & E are β-1 integrin staining; Panel C & F are the overlay of the first two images.

In contrast, Asm-deficient T lymphocytes from EAE-immunized mice failed to form ceramide-enriched membrane platforms and β-1 integrin clusters; β-1 integrin remained uniformly distributed over the plasma membrane (Fig. 4.15). These findings indicate that lymphocyte Asm is required for β-1 integrin clustering and function and the resultant T-cell adhesion.

4.5.3   Transmigration

Based on our adhesion data, which showed a crucial role for Asm in the adhesion of lymphocytes to a bEnd.3 monolayer *in vitro*, and that Asm deficient mice were devoid of inflammatory infiltrates, we hypothesized that transmigration would also be reduced in Asm -/- cells in an *in vitro* assay. Using the same endothelial cell line as in the adhesion assays, we plated Transwells to create a monolayer and applied wt or Asm -/- cells to the upper compartment. Analysis of cell counts from the lower compartment after 4 hours, however, did not reveal any significant difference between wt and Asm -/- lymphocytes (Fig. 4.16).
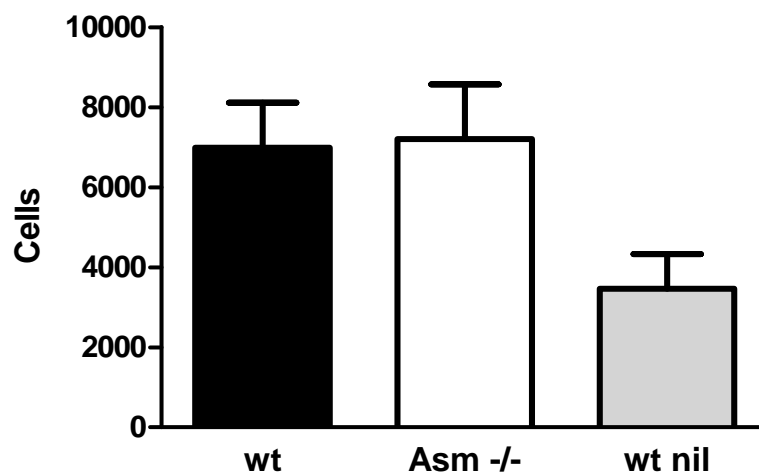

Figure 4.16 Asm deficiency does reduce transmigration of lymphocytes *in vitro*. Transmigration across a bEnd.3 monolayer was not significantly different between wt and Asm deficient lymphocytes, or compared with non-immunized control ($p \geq 0.05$, one-way ANOVA). Shown are means + SEM for 17 wt and 12 Asm -/- mice.

4.6   Functional blockade of Asm with amitriptyline rescues wt mice from EAE and prevents lymphocyte adhesion

As a therapeutic approach, we treated EAE-immunized wt mice twice daily with the potent Asm inhibitor amitriptyline (Kornhuber et al., 2010) administered i.p. at a dose of 10 mg/kg body weight starting on day 1 or day 10, respectively, after immunization to test whether amitriptyline blocks the development or clinical manifestation of the late effector phase of EAE, modeling the clinical situation. Due to treatment issues with the C57Bl6/J mice resulting in cardiac failure, we instead used SJL mice immunized with PLP for the amitriptyline experiments.

Amitriptyline protected mice from the development of clinical EAE symptoms (Fig. 4.17). The number of affected mice was reduced by 51% when treatment started at day 1 and was even reduced by 28% when amitriptyline administration was started at day 10 after immunization (Fig. 4.17) indicating that amitriptyline can also block the effector phase of EAE development.
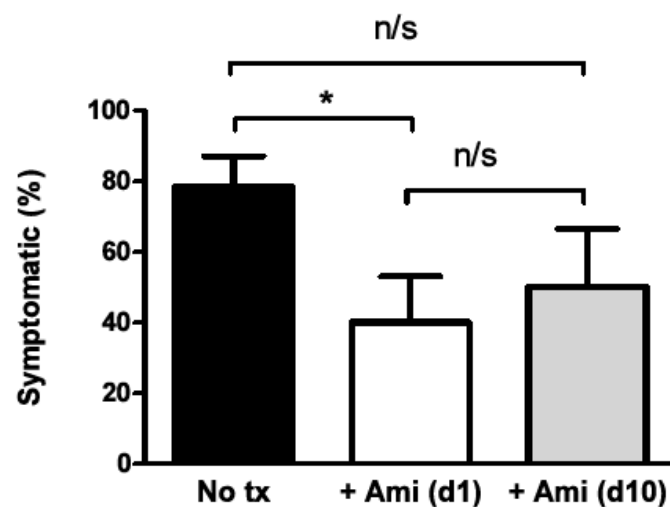
Figure 4.17 Pharmacologic inhibition of Asm with amitriptyline provides protection against active EAE. SJL mice were actively immunized for EAE and treated with amitriptyline starting on day 1 (n=15) or day 10 (n=10) and compared with control (No tx) animals injected with distilled water (n=23). Shown is the percentage of mice with clinical symptoms. Amitriptyline treatment significantly reduced the number of diseased mice at day 1 (*p ≤ 0.05, t-test) but not when administered at day 10 (n/s p ≥ 0.05, one-way ANOVA). n/s = not significant.

Immunohistochemical analysis of spinal cord samples confirmed the complete absence of leukocytes in amitriptyline-treated mice and, thus, the protective effect of amitriptyline administration through Asm inhibition (Fig. 4.18).
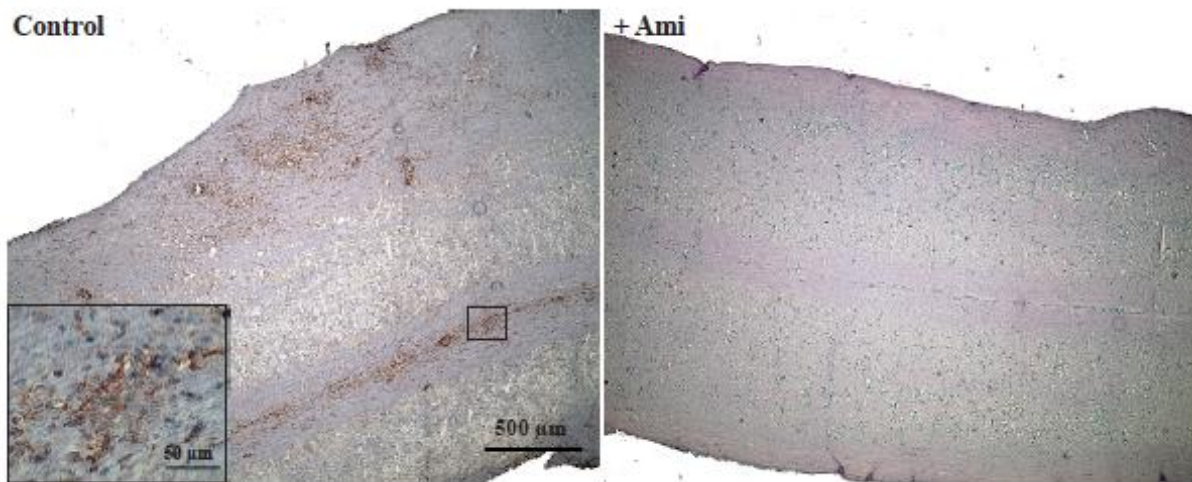
Figure 4.18 Pharmacologic inhibition of Asm with amitriptyline reduces inflammatory infiltration. Immunohistochemistry staining with CD45 confirms reduced leukocyte infiltration in SJL mice treated with amitriptyline in spinal cord compared to control mice where significant infiltration is prevalent. The reduction in inflammatory infiltration corroborates the reduced clinical score. Shown are typical frozen sections (6 μm) from a control mouse at peak of disease and an amitriptyline treated mouse with a clinical score of 0 taken at the same time point.

Adhesion analysis of amitriptyline treated wt lymphocytes showed an adhesion blockade with the same extent as Asm deficient lymphocytes (Fig. 4.19). The finding that amitriptyline did not further reduce the adhesion of Asm-deficient lymphocytes to bEnd.3 cells hints towards a specific targeting of Asm by amitriptyline in this context (Fig. 4.20).
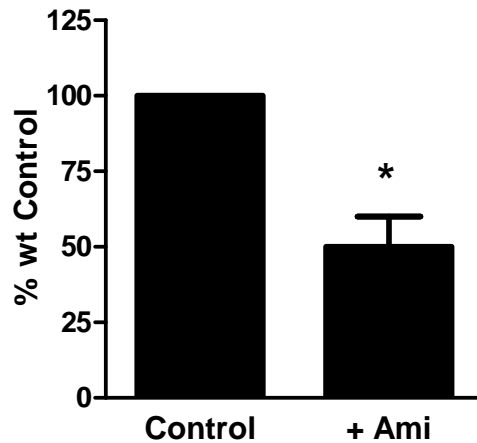
Figure 4.19 Pharmacologic inhibition of Asm with amitriptyline inhibits adhesion of wt lymphocytes. In vitro adhesion assays showed a significant reduction in the adhesion of wt lymphocytes to bEnd.3 cells when treated with 10 μM amitriptyline. Shown are means + SEM of wt control (n=10) and wt treated with amitriptyline (n=10). *$p \leq 0.05$, t-test.
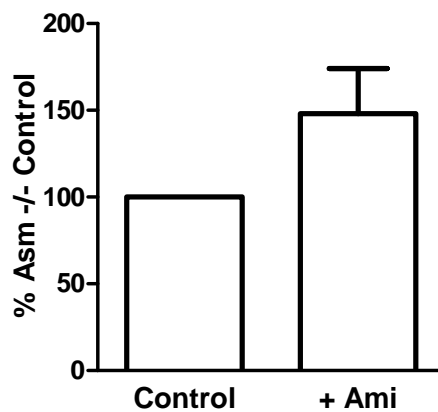
Figure 4.20 Pharmacologic inhibition of Asm with amitriptyline in Asm deficient lymphocytes does not significantly decrease adhesion. In vitro adhesion assays showed no significant reduction in the adhesion of Asm -/- lymphocytes to bEnd.3 cells when treated with 10 μM amitriptyline. Shown are means + SEM of Asm -/- control (n=10) and Asm -/- treated with amitriptyline (n=10). $p \geq 0.05$, t-test.

5 Discussion

MS is a chronic, demyelinating inflammatory disease of the CNS characterized by CNS-specific immune cell infiltration from the peripheral vascular compartment, and nervous tissue damage, namely myelin degradation and axonal injury with subsequent neuronal loss (Alvarez et al., 2011). Central to this disease pathway is the adhesion of lymphocytes to endothelial cells and the ultimate migration of these lymphocytes from the peripheral circulation across the BBB. The adhesion and transmigration of lymphocytes across the endothelium is a complex process involving interactions between complementary adhesion molecules on the surfaces of lymphocytes and endothelial cells (Engelhardt and Ransohoff, 2005). In this study, we demonstrate that genetic or pharmacological inhibition of Asm protects against experimental MS. Specifically, T lymphocytes lacking Asm activity either through genetic Asm deficiency or pharmacological Asm inhibition by administration of amitriptyline show a reduced clustering of integrins resulting in reduced adhesion and disruption of tight junctions. Thus, Asm controls key steps in the neuro-inflammatory cascade leading to neuronal injury during MS.

5.1 Asm is essential for EAE disease pathogenesis

In our study, we observed that the loss of Asm activity through genetic knockout served to protect against disease development in a mouse model of EAE in stark contrast with wild-type mice, which were consistently sick with significantly worse clinical outcomes. Interestingly, an increased production of ceramide and Asm has been found in astrocytes, particularly in the astrocytic endfeet, from MS lesion brain tissue (van Doorn et al., 2012) suggesting a role of Asm in MS pathology. We were able to show that mice lacking clinical disease manifestations were also devoid of inflammatory infiltration, correlating histology with clinical score. Our results are consistent with previous work in EAE, which showed that inflammation and lesion formation is strongly correlated with disease severity (Recks et al., 2011). We were able to abolish this protection by transplanting wt bone marrow into Asm-deficient mice. These results suggest an important role of Asm activity in the leukocyte in initiating EAE pathogenesis.

5.2 Asm activity is involved in the breakdown of the blood-brain barrier

As a potential mechanism, we found that Asm activity is involved in the breakdown of the BBB during EAE. BBB breakdown has been shown to be the crucial step in MS pathology, preceding neurologic disease in MS patients (Kermode et al., 1990). Using the method of injecting Evans Blue dye (EBD) intravascularly to assess BBB integrity, we were able to show significant EBD leakage into the spinal cord parenchyma, both visually through histologic examination as well as with quantitative spectrophotometric analysis in wt mice. Our results are corroborated by previous studies showing a correlation between disease severity and degree of BBB breakdown (Fabis et al., 2007) with a more than 10-fold increase compared to control (non-immunized) animals. In concordance with this data, we demonstrate that Asm -/- mice, lacking clinical and histologic manifestations of EAE disease, had maintained BBB integrity with no leakage of EBD into the spinal cord parenchyma when assessed visually. This is in line with a recent report which found a decrease in BBB integrity in an *in vitro* endothelial cell layer treated with Asm (van Doorn et al., 2012). Furthermore, they were able to replicate their findings of decreased barrier function using conditioned medium from reactive inflammatory astrocytes (which produce increased amounts of ceramide and Asm) from the brains of MS patients indicating a direct role of Asm on BBB maintenance.

The spectrophotometric analysis of spinal cord homogenate showed some leakage of EBD in Asm -/- mice, though significantly less than wt, despite the lack of clinical manifestations and visual evidence of EBD infiltration. However, this minor leakage may have been artefact of EBD remaining in microvessels or a direct effect of pertussis toxin administration, which has been shown to induce changes in permeability in an in vitro assay (Bennett et al., 2010). In addition to showing decreased BBB permeability in mice deficient for the Asm enzyme, we were also able to demonstrate a concordant decrease in destruction of tight junctions. Specifically, we showed vessel ZO-1 and claudin-5 abnormalities in clinically ill wt mice, and a preservation of these tight junctions in Asm -/- mice. ZO-1 disruption has been previously shown to correlate with EAE disease severity and infiltration/lesion site in mouse spinal cord (Bennett et al., 2010). Recently, claudin-5 disruption was also demonstrated during EAE with a loss of normal junctional staining patterns. The reasons for tight junction breakdown are not fully understood, though claudin-5 is potentially internalized as it is co-expressed with an autophagosomal marker (Errede et al., 2012).

5.3 Asm is involved in the lymphocyte adhesion pathway

We demonstrate that Asm is important in the lymphocyte adhesion pathway during EAE. As an immune-mediated disease, EAE pathogenesis is highly dependent upon the interaction of lymphocytes with the endothelium in the central nervous system. This interaction involves multiple steps, including rolling, chemokine production and firm adhesion through LFA-1 and $\alpha_4\beta_1$ on lymphocytes binding with their endothelial counterparts, ICAM-1 and VCAM-1 (Laschinger et al., 2002), and final transmigration of cells. Of these multiple steps, firm adhesion seems to be a crucial step in EAE pathogenesis. Using an *in vitro* adhesion assay we were able to demonstrate a significant reduction in adhesion in Asm-deficient T cells compared with wt T cells. Furthermore, in line with previous research regarding the importance of integrins in leukocyte adhesion, we were also able to reverse the effects of Asm-deficiency on adhesion by applying Mn^{2+}. The divalent cation, Mn^{2+}, has been previously shown to directly act upon LFA-1 and strongly promote binding with ICAM-1 (Dransfield et al., 1992). Additionally, It was previously demonstrated that α-4 integrin is important in EAE (Baron et al., 1993) and that blocking α-4 with the monoclonal antibody, natalizumab, was able to suppress EAE in an animal model (Kent et al., 1995). Furthermore, natalizumab was effective in clinical studies in reducing relapse rates and disease progression (Polman et al., 2006).

5.4 Asm activity does not affect integrin expression

We demonstrate that integrin expression levels are not affected by Asm activity; there was no significant difference in β-1 or β-7 integrin expression between wt and Asm-deficient cells. This was true regardless of whether the cells were isolated from lymph node or spleen. It has been previously shown that β-1 integrin is important in the adhesion of encephalitogenic T cell blasts in EAE (Laschinger and Engelhardt, 2000). In fact, the deletion of β-1 integrin from the entire encephalitogenic T lymphocyte population was able to completely prevent EAE disease induction (Bauer et al., 2009). However, integrins are normally constitutively expressed on leukocytes but kept in a low affinity state (Carman and Springer, 2003). In order to firmly bind to their respective endothelial ligands, leukocyte integrins must undergo *in situ* modulation to develop high avidity (Alon and Feigelson, 2002). Our results indicate that integrin expression is not the key factor in the protection of Asm-deficient mice from EAE, however, a lack of change in expression does not rule out a change in avidity.

5.5   Asm affects adhesion by modulating ceramide raft formation

In collaboration with the group of Dr. E. Gulbins, we demonstrate that clustering of β-1 integrin, increasing ligand avidity, is mediated by ceramide-enriched membrane platforms, which is, thus, integral to leukocyte adhesion and EAE disease pathogenesis. For a number of years, ceramide has been known to alter the biophysical characteristics of cell membranes. Ceramide molecules spontaneously fuse to form membrane micro-domains (Kolesnick et al., 2000), which can then go on to form macro-domains, called ceramide-enriched membrane platforms. These ceramide-enriched membrane platforms have been shown to be essential for the clustering of activated receptors (Grassme et al., 2001b).

We observed the formation of ceramide rafts and clustering of β-1 integrin molecules within those rafts in activated, antigen-specific wt lymphocytes. Receptor clustering results in a high density of receptor molecules, consequently permitting and amplifying signal transduction by this receptor (Grassme et al., 2001a). The precise molecular mechanisms of ceramide-mediated receptor clustering are unknown, however, it is hypothesized that the length of the transmembrane domain and the conformation of a receptor molecule may determine its ability to assemble in ceramide membrane domains (Zhang et al., 2009).

Furthermore, we were able to demonstrate that Asm -/- lymphocytes were neither able to form ceramide rafts nor were they able to cluster β-1 integrin molecules. This is in line with previous studies which showed that Asm is important in the release of ceramide in sphingolipid-rich rafts and, consequently, clustering of CD40 (Grassme et al., 2002b). Asm deficiency was also sufficient to prevent CD95 clustering and apoptosis (Grassme et al., 2001a). These results explain why there was no change in expression of β-1 integrin despite its previously demonstrated role in EAE development (Bauer et al., 2009). VLA-4, as well as LFA-1 mediated cell adhesion is regulated by receptor clustering (van Kooyk et al., 1999, Grabovsky et al., 2000) the absence of which, in our study, would account for the decreased adhesion of leukocytes and the protection from EAE.

5.6 Asm does not influence transendothelial migration, proliferation or cytokine expression

Interestingly, we were unable to demonstrate a significant difference in transendothelial migration of T lymphocytes between Asm -/- and wt cells, despite the significant decrease in lymphocyte adhesion. In contrast with our findings, van Doorn et al. (van Doorn et al., 2012) recently demonstrated an increase in transmigration of monocytes across an endothelial monolayer when treated with Asm or a conditioned medium from reactive inflammatory astrocytes, which they demonstrate can produce increased ceramide and Asm. However, our adhesion results indicate a direct effect of the $\alpha_4\beta_1$ integrin which has been previously shown to have no effect on transendothelial migration *in vitro* (Laschinger and Engelhardt, 2000), corroborating our findings.

Likewise, we also found that Asm-deficiency had no effect on proliferation of T cells or cytokine production in lymphocytes. Bauer et al. (Bauer et al., 2009) previously demonstrated that β-1 integrin was also not involved in T cell proliferation or production of cytokines during EAE. This is highly beneficial as this suggests that immunosuppression is very unlikely in a clinical setting when Asm activity is inhibited. Of note, Asm has been found to trigger release of microparticles containing IL-1β from glial cells (Bianco et al., 2009). This data does not necessarily contradict our findings as we assessed cytokine expression in lymphocytes harvested from lymph node and spleen, but did not directly assess cytokine expression of T cells that had adhered to or infiltrated across the BBB, nor did we directly assess cytokine release.

5.7 Pharmacologic inhibition of Asm affords protection in EAE

Numerous pharmacologic agents have been found to inhibit Asm activity in recent years, including amitriptyline, fluoxetine, sertraline, desipramine and amlodipine amongst others (Kornhuber et al., 2010). These drugs belong to a class of drugs known as FIASMA's (functional inhibitor of acid sphingomyelinase) and are all weak bases. Specifically in our study we assessed amitriptyline, a well-known antidepressant that has been used in clinical practice since 1961 (Fangmann et al., 2008). Amitriptyline, as well as the other FIASMA drugs, acts by competitive inhibition of Asm, displacing the enzyme from lysosomal membranes, with subsequent degradation of the enzyme (Kornhuber et al., 2008). Consequently, amitriptyline only inhibits 60% to 80% of Asm activity (Teichgraber et al.,

2008) and, thus, does not cause the manifestations of Niemann-Pick disease, which requires less than 10% of mean normal enzyme activity (van Diggelen et al., 2005). This incomplete inhibition of Asm activity by amitriptyline also explains why long-term treatment of patients with major depression does not result in severe side effects, such as immunodeficiency.

Our study shows that treatment with amitriptyline significantly reduces clinical disease in a mouse model of EAE, which mimics our findings in mice with Asm genetic deficiency. Furthermore, amitriptyline significantly decreases acute adhesion of T-lymphocytes in an *in vitro* assay to the same degree as genetic knockout of the enzyme. In 2004, Göggel et al. showed an Asm-dependent increase in vascular permeability in isolated lung vessels treated with platelet-activating factor (Goggel et al., 2004). Our observation of reduced lymphocyte adhesion taken in conjunction with decreased vascular permeability is sufficient to explain the significant reduction in the development of EAE. This result would be equivalent and, in some cases, superior to previously described immunomodulating MS therapies, without the adverse side effects (Espinosa and Berger, 2011, Sorensen et al., 2012, Smith et al., 2010). For instance, an α-4 integrin antibody when given before disease induction, was able to reduce the number of symptomatic mice by 75% (Yednock et al., 1992); a reduction that we were also able to achieve with amitriptyline. However, when the α-4 integrin antibody was given after disease induction, the effect was diminished and served to only delay clinical symptoms but not prevent them (Kent et al., 1995). In contrast, when we administered amitriptyline 10 days after disease induction we were still able to observe a decrease in clinical disease expression.

Therefore, given the long-term experience and clinical safety of amitriptyline and the present results with EAE, amitriptyline (or another FIASMA), is a very good candidate for a clinical study involving patients with MS. Indeed, a clinical study of MS patients treated with fluoxetine has already shown a reduction in MRI lesion progression, though the patients were only followed for 24 weeks (Mostert et al., 2008). Interestingly, FTY720 (the S1P receptor agonist) has been demonstrated to inhibit Asm in a manner similar to the FIASMA drug group (Dawson and Qin, 2011). Recently, FTY720 was also found to decrease Asm enzyme expression and subsequent ceramide formation in reactive human astrocytes harvested from MS brain lesions (van Doorn et al., 2012). FTY720 has been successfully used to treat MS patients (Kappos et al., 2010) and inhibits T cell infiltration in an animal model of EAE

(Kataoka et al., 2005). These studies are in concordance with our work and support our finding that Asm is an important factor in EAE pathogenesis.

In summary, we demonstrate the role of Asm in a mouse model of MS. We show that Asm is a key enzyme in lymphocyte/endothelial cell adhesion by modulating ceramide raft formation and the subsequent clustering of adhesion integrins, specifically β-1 integrin. Loss of Asm enzyme activity reduces lipid platform creation, which results in decreased integrin clustering leading to loss of adhesion capability. This decrease in adhesion serves to protect against EAE disease pathogenesis, and mice lacking the gene for Asm were consistently free of clinical disease and histopathologic markers of disease, including inflammatory infiltration and BBB breakdown. Furthermore, pharmacologic inhibition of Asm by amitriptyline was effective in protecting against EAE. Our study contributes to the understanding of MS pathogenesis and provides a good candidate for the treatment of MS in the clinical setting.

References

ALON, R. & FEIGELSON, S. 2002. From rolling to arrest on blood vessels: leukocyte tap dancing on endothelial integrin ligands and chemokines at sub-second contacts. *Semin Immunol,* 14**,** 93-104.

ALT, C., LASCHINGER, M. & ENGELHARDT, B. 2002. Functional expression of the lymphoid chemokines CCL19 (ELC) and CCL 21 (SLC) at the blood-brain barrier suggests their involvement in G-protein-dependent lymphocyte recruitment into the central nervous system during experimental autoimmune encephalomyelitis. *Eur J Immunol,* 32**,** 2133-44.

ALVAREZ, J. I., CAYROL, R. & PRAT, A. 2011. Disruption of central nervous system barriers in multiple sclerosis. *Biochim Biophys Acta,* 1812**,** 252-64.

ASCHERIO, A. & MUNGER, K. L. 2007. Environmental risk factors for multiple sclerosis. Part I: the role of infection. *Ann Neurol,* 61**,** 288-99.

BABICH, V., KNIPE, L., HEWLETT, L., MELI, A., DEMPSTER, J., HANNAH, M. J. & CARTER, T. 2009. Differential effect of extracellular acidosis on the release and dispersal of soluble and membrane proteins secreted from the Weibel-Palade body. *J Biol Chem,* 284**,** 12459-68.

BARON, J. L., MADRI, J. A., RUDDLE, N. H., HASHIM, G. & JANEWAY, C. A., JR. 1993. Surface expression of alpha 4 integrin by CD4 T cells is required for their entry into brain parenchyma. *J Exp Med,* 177**,** 57-68.

BARTH, B. M., GUSTAFSON, S. J. & KUHN, T. B. 2012. Neutral sphingomyelinase activation precedes NADPH oxidase-dependent damage in neurons exposed to the proinflammatory cytokine tumor necrosis factor-alpha. *J Neurosci Res,* 90**,** 229-42.

BAUER, M., BRAKEBUSCH, C., COISNE, C., SIXT, M., WEKERLE, H., ENGELHARDT, B. & FASSLER, R. 2009. Beta1 integrins differentially control extravasation of inflammatory cell subsets into the CNS during autoimmunity. *Proc Natl Acad Sci U S A,* 106**,** 1920-5.

BECHER, B., BECHMANN, I. & GRETER, M. 2006. Antigen presentation in autoimmunity and CNS inflammation: how T lymphocytes recognize the brain. *J Mol Med (Berl),* 84**,** 532-43.

BENNETT, J., BASIVIREDDY, J., KOLLAR, A., BIRON, K. E., REICKMANN, P., JEFFERIES, W. A. & MCQUAID, S. 2010. Blood-brain barrier disruption and enhanced vascular permeability in the multiple sclerosis model EAE. *J Neuroimmunol,* 229**,** 180-91.

BHATIA, R., MATSUSHITA, K., YAMAKUCHI, M., MORRELL, C. N., CAO, W. & LOWENSTEIN, C. J. 2004. Ceramide triggers Weibel-Palade body exocytosis. *Circ Res,* 95**,** 319-24.

BIANCO, F., PERROTTA, C., NOVELLINO, L., FRANCOLINI, M., RIGANTI, L., MENNA, E., SAGLIETTI, L., SCHUCHMAN, E. H., FURLAN, R., CLEMENTI, E., MATTEOLI, M. & VERDERIO, C. 2009. Acid sphingomyelinase activity triggers microparticle release from glial cells. *EMBO J,* 28**,** 1043-54.

BIELEKOVA, B. & MARTIN, R. 2004. Development of biomarkers in multiple sclerosis. *Brain,* 127**,** 1463-78.

BOUCHER, L. M., WIEGMANN, K., FUTTERER, A., PFEFFER, K., MACHLEIDT, T., SCHUTZE, S., MAK, T. W. & KRONKE, M. 1995. CD28 signals through acidic sphingomyelinase. *J Exp Med,* 181**,** 2059-68.

BRADY, R. O., KANFER, J. N., MOCK, M. B. & FREDRICKSON, D. S. 1966. The metabolism of sphingomyelin. II. Evidence of an enzymatic deficiency in Niemann-Pick diseae. *Proc Natl Acad Sci U S A,* 55**,** 366-9.

BRONNUM-HANSEN, H., KOCH-HENRIKSEN, N. & STENAGER, E. 2004. Trends in survival and cause of death in Danish patients with multiple sclerosis. *Brain,* 127**,** 844-50.

BURNS, A. R., BOWDEN, R. A., ABE, Y., WALKER, D. C., SIMON, S. I., ENTMAN, M. L. & SMITH, C. W. 1999. P-selectin mediates neutrophil adhesion to endothelial cell borders. *J Leukoc Biol,* 65**,** 299-306.

CARMAN, C. V. & SPRINGER, T. A. 2003. Integrin avidity regulation: are changes in affinity and conformation underemphasized? *Curr Opin Cell Biol,* 15**,** 547-56.

CLANET, M. 2008. Jean-Martin Charcot. 1825 to 1893. *Int MS J,* 15**,** 59-61.

COMPSTON, A. & COLES, A. 2008. Multiple sclerosis. *Lancet,* 372**,** 1502-17.

DAWSON, G. & QIN, J. 2011. Gilenya (FTY720) inhibits acid sphingomyelinase by a mechanism similar to tricyclic antidepressants. *Biochem Biophys Res Commun,* 404**,** 321-3.

DIMANCHE-BOITREL, M. T., MEURETTE, O., REBILLARD, A. & LACOUR, S. 2005. Role of early plasma membrane events in chemotherapy-induced cell death. *Drug Resist Updat,* 8**,** 5-14.

DRANSFIELD, I., CABANAS, C., CRAIG, A. & HOGG, N. 1992. Divalent cation regulation of the function of the leukocyte integrin LFA-1. *J Cell Biol,* 116**,** 219-26.

DYMENT, D. A., SADOVNICK, A. D. & EBERS, G. C. 1997. Genetics of multiple sclerosis. *Hum Mol Genet,* 6**,** 1693-8.

ENGELHARDT, B. 2006. Molecular mechanisms involved in T cell migration across the blood-brain barrier. *J Neural Transm,* 113**,** 477-85.

ENGELHARDT, B. & RANSOHOFF, R. M. 2005. The ins and outs of T-lymphocyte trafficking to the CNS: anatomical sites and molecular mechanisms. *Trends Immunol,* 26**,** 485-95.

ENGELHARDT, B., VESTWEBER, D., HALLMANN, R. & SCHULZ, M. 1997. E- and P-selectin are not involved in the recruitment of inflammatory cells across the blood-brain barrier in experimental autoimmune encephalomyelitis. *Blood,* 90**,** 4459-72.

ERREDE, M., GIROLAMO, F., FERRARA, G., STRIPPOLI, M., MORANDO, S., BOLDRIN, V., RIZZI, M., UCCELLI, A., PERRIS, R., BENDOTTI, C., SALMONA, M., RONCALI, L. & VIRGINTINO, D. 2012. Blood-Brain Barrier Alterations in the Cerebral Cortex in Experimental Autoimmune Encephalomyelitis. *J Neuropathol Exp Neurol,* 71**,** 840-854.

ESPINOSA, P. S. & BERGER, J. R. 2011. Delayed fingolimod-associated asystole. *Mult Scler,* 17**,** 1387-9.

FABIS, M. J., SCOTT, G. S., KEAN, R. B., KOPROWSKI, H. & HOOPER, D. C. 2007. Loss of blood-brain barrier integrity in the spinal cord is common to experimental allergic encephalomyelitis in knockout mouse models. *Proc Natl Acad Sci U S A,* 104**,** 5656-61.

FANGMANN, P., ASSION, H. J., JUCKEL, G., GONZALEZ, C. A. & LOPEZ-MUNOZ, F. 2008. Half a century of antidepressant drugs: on the clinical introduction of monoamine oxidase inhibitors, tricyclics, and tetracyclics. Part II: tricyclics and tetracyclics. *J Clin Psychopharmacol,* 28**,** 1-4.

FERLINZ, K., HURWITZ, R., VIELHABER, G., SUZUKI, K. & SANDHOFF, K. 1994. Occurrence of two molecular forms of human acid sphingomyelinase. *Biochem J,* 301 (Pt 3)**,** 855-62.

FROHMAN, E. M., RACKE, M. K. & RAINE, C. S. 2006. Multiple sclerosis--the plaque and its pathogenesis. *N Engl J Med,* 354**,** 942-55.

FUJINAMI, R. S., VON HERRATH, M. G., CHRISTEN, U. & WHITTON, J. L. 2006. Molecular mimicry, bystander activation, or viral persistence: infections and autoimmune disease. *Clin Microbiol Rev,* 19**,** 80-94.

GALEA, I., BERNARDES-SILVA, M., FORSE, P. A., VAN ROOIJEN, N., LIBLAU, R. S. & PERRY, V. H. 2007. An antigen-specific pathway for CD8 T cells across the blood-brain barrier. *J Exp Med,* 204**,** 2023-30.

GATT, S. 1963. Enzymic Hydrolysis and Synthesis of Ceramides. *J Biol Chem,* 238**,** 3131-3.

GOETZL, E. J. & GRALER, M. H. 2004. Sphingosine 1-phosphate and its type 1 G protein-coupled receptor: trophic support and functional regulation of T lymphocytes. *J Leukoc Biol,* 76**,** 30-5.

GOETZL, E. J. & ROSEN, H. 2004. Regulation of immunity by lysosphingolipids and their G protein-coupled receptors. *J Clin Invest,* 114**,** 1531-7.

GOGGEL, R., WINOTO-MORBACH, S., VIELHABER, G., IMAI, Y., LINDNER, K., BRADE, L., BRADE, H., EHLERS, S., SLUTSKY, A. S., SCHUTZE, S., GULBINS, E. & UHLIG, S. 2004. PAF-mediated pulmonary edema: a new role for acid sphingomyelinase and ceramide. *Nat Med,* 10**,** 155-60.

GRABOVSKY, V., FEIGELSON, S., CHEN, C., BLEIJS, D. A., PELED, A., CINAMON, G., BALEUX, F., ARENZANA-SEISDEDOS, F., LAPIDOT, T., VAN KOOYK, Y., LOBB, R. R. & ALON, R. 2000. Subsecond induction of alpha4 integrin clustering by immobilized chemokines stimulates leukocyte tethering and rolling on endothelial vascular cell adhesion molecule 1 under flow conditions. *J Exp Med,* 192**,** 495-506.

GRASSME, H., BOCK, J., KUN, J. & GULBINS, E. 2002a. Clustering of CD40 ligand is required to form a functional contact with CD40. *J Biol Chem,* 277**,** 30289-99.

GRASSME, H., JEKLE, A., RIEHLE, A., SCHWARZ, H., BERGER, J., SANDHOFF, K., KOLESNICK, R. & GULBINS, E. 2001a. CD95 signaling via ceramide-rich membrane rafts. *J Biol Chem,* 276**,** 20589-96.

GRASSME, H., JENDROSSEK, V., BOCK, J., RIEHLE, A. & GULBINS, E. 2002b. Ceramide-rich membrane rafts mediate CD40 clustering. *J Immunol,* 168**,** 298-307.

GRASSME, H., SCHWARZ, H. & GULBINS, E. 2001b. Molecular mechanisms of ceramide-mediated CD95 clustering. *Biochem Biophys Res Commun,* 284**,** 1016-30.

GRETER, M., HEPPNER, F. L., LEMOS, M. P., ODERMATT, B. M., GOEBELS, N., LAUFER, T., NOELLE, R. J. & BECHER, B. 2005. Dendritic cells permit immune invasion of the CNS in an animal model of multiple sclerosis. *Nat Med,* 11**,** 328-34.

GULBINS, E. & LI, P. L. 2006. Physiological and pathophysiological aspects of ceramide. *Am J Physiol Regul Integr Comp Physiol,* 290**,** R11-26.

HAWKES, C. H. & MACGREGOR, A. J. 2009. Twin studies and the heritability of MS: a conclusion. *Mult Scler,* 15**,** 661-7.

HAWKINS, B. T. & DAVIS, T. P. 2005. The blood-brain barrier/neurovascular unit in health and disease. *Pharmacol Rev,* 57**,** 173-85.

HENRY, B., MOLLER, C., DIMANCHE-BOITREL, M. T., GULBINS, E. & BECKER, K. A. 2011. Targeting the ceramide system in cancer. *Cancer Lett*.

HURWITZ, R., FERLINZ, K. & SANDHOFF, K. 1994. The tricyclic antidepressant desipramine causes proteolytic degradation of lysosomal sphingomyelinase in human fibroblasts. *Biol Chem Hoppe Seyler,* 375**,** 447-50.

JACOBS, L. D., COOKFAIR, D. L., RUDICK, R. A., HERNDON, R. M., RICHERT, J. R., SALAZAR, A. M., FISCHER, J. S., GOODKIN, D. E., GRANGER, C. V., SIMON, J. H., ALAM, J. J., BARTOSZAK, D. M., BOURDETTE, D. N., BRAIMAN, J., BROWNSCHEIDLE, C. M., COATS, M. E., COHAN, S. L., DOUGHERTY, D. S., KINKEL, R. P., MASS, M. K., MUNSCHAUER, F. E., 3RD, PRIORE, R. L., PULLICINO, P. M., SCHEROKMAN, B. J., WHITHAM, R. H. & ET AL. 1996. Intramuscular interferon beta-1a for disease progression in relapsing multiple sclerosis. The Multiple Sclerosis Collaborative Research Group (MSCRG). *Ann Neurol,* 39**,** 285-94.

JANA, A. & PAHAN, K. 2007. Oxidative stress kills human primary oligodendrocytes via neutral sphingomyelinase: implications for multiple sclerosis. *J Neuroimmune Pharmacol,* 2**,** 184-93.

JANA, A. & PAHAN, K. 2010. Sphingolipids in multiple sclerosis. *Neuromolecular Med,* 12**,** 351-61.

JOHNSON, K. P., BROOKS, B. R., COHEN, J. A., FORD, C. C., GOLDSTEIN, J., LISAK, R. P., MYERS, L. W., PANITCH, H. S., ROSE, J. W. & SCHIFFER, R. B. 1995. Copolymer 1 reduces relapse rate and improves disability in relapsing-remitting multiple sclerosis: results of a phase III multicenter, double-blind placebo-controlled trial. The Copolymer 1 Multiple Sclerosis Study Group. *Neurology,* 45**,** 1268-76.

KANTER, J. L., NARAYANA, S., HO, P. P., CATZ, I., WARREN, K. G., SOBEL, R. A., STEINMAN, L. & ROBINSON, W. H. 2006. Lipid microarrays identify key mediators of autoimmune brain inflammation. *Nat Med,* 12**,** 138-43.

KAPPOS, L., ANTEL, J., COMI, G., MONTALBAN, X., O'CONNOR, P., POLMAN, C. H., HAAS, T., KORN, A. A., KARLSSON, G. & RADUE, E. W. 2006. Oral fingolimod (FTY720) for relapsing multiple sclerosis. *N Engl J Med,* 355**,** 1124-40.

KAPPOS, L., RADUE, E. W., O'CONNOR, P., POLMAN, C., HOHLFELD, R., CALABRESI, P., SELMAJ, K., AGOROPOULOU, C., LEYK, M., ZHANG-AUBERSON, L. & BURTIN, P. 2010. A placebo-controlled trial of oral fingolimod in relapsing multiple sclerosis. *N Engl J Med,* 362**,** 387-401.

KATAOKA, H., SUGAHARA, K., SHIMANO, K., TESHIMA, K., KOYAMA, M., FUKUNARI, A. & CHIBA, K. 2005. FTY720, sphingosine 1-phosphate receptor modulator, ameliorates experimental autoimmune encephalomyelitis by inhibition of T cell infiltration. *Cell Mol Immunol,* 2**,** 439-48.

KENT, S. J., KARLIK, S. J., CANNON, C., HINES, D. K., YEDNOCK, T. A., FRITZ, L. C. & HORNER, H. C. 1995. A monoclonal antibody to alpha 4 integrin suppresses and reverses active experimental allergic encephalomyelitis. *J Neuroimmunol,* 58**,** 1-10.

KERFOOT, S. M. & KUBES, P. 2002. Overlapping roles of P-selectin and alpha 4 integrin to recruit leukocytes to the central nervous system in experimental autoimmune encephalomyelitis. *J Immunol,* 169**,** 1000-6.

KERMODE, A. G., THOMPSON, A. J., TOFTS, P., MACMANUS, D. G., KENDALL, B. E., KINGSLEY, D. P., MOSELEY, I. F., RUDGE, P. & MCDONALD, W. I. 1990. Breakdown of the blood-brain barrier precedes symptoms and other MRI signs of new lesions in multiple sclerosis. Pathogenetic and clinical implications. *Brain,* 113 (Pt 5)**,** 1477-89.

KOLESNICK, R. N., GONI, F. M. & ALONSO, A. 2000. Compartmentalization of ceramide signaling: physical foundations and biological effects. *J Cell Physiol,* 184**,** 285-300.

KOLZER, M., WERTH, N. & SANDHOFF, K. 2004. Interactions of acid sphingomyelinase and lipid bilayers in the presence of the tricyclic antidepressant desipramine. *FEBS Lett,* 559**,** 96-8.

KORNHUBER, J., TRIPAL, P., REICHEL, M., MUHLE, C., RHEIN, C., MUEHLBACHER, M., GROEMER, T. W. & GULBINS, E. 2010. Functional Inhibitors of Acid Sphingomyelinase (FIASMAs): a novel pharmacological group of drugs with broad clinical applications. *Cell Physiol Biochem,* 26**,** 9-20.

KORNHUBER, J., TRIPAL, P., REICHEL, M., TERFLOTH, L., BLEICH, S., WILTFANG, J. & GULBINS, E. 2008. Identification of new functional inhibitors of acid sphingomyelinase using a structure-property-activity relation model. *J Med Chem,* 51**,** 219-37.

KUNZ, M. & IBRAHIM, S. M. 2009. Cytokines and cytokine profiles in human autoimmune diseases and animal models of autoimmunity. *Mediators Inflamm,* 2009**,** 979258.

LASCHINGER, M. & ENGELHARDT, B. 2000. Interaction of alpha4-integrin with VCAM-1 is involved in adhesion of encephalitogenic T cell blasts to brain endothelium but not in their transendothelial migration in vitro. *J Neuroimmunol,* 102**,** 32-43.

LASCHINGER, M., VAJKOCZY, P. & ENGELHARDT, B. 2002. Encephalitogenic T cells use LFA-1 for transendothelial migration but not during capture and initial adhesion strengthening in healthy spinal cord microvessels in vivo. *Eur J Immunol,* 32**,** 3598-606.

LUCAS, S. M., ROTHWELL, N. J. & GIBSON, R. M. 2006. The role of inflammation in CNS injury and disease. *Br J Pharmacol,* 147 Suppl 1**,** S232-40.

LUO, C., WANG, K., LIU DE, Q., LI, Y. & ZHAO, Q. S. 2008. The functional roles of lipid rafts in T cell activation, immune diseases and HIV infection and prevention. *Cell Mol Immunol,* 5**,** 1-7.

MILO, R. & KAHANA, E. 2010. Multiple sclerosis: geoepidemiology, genetics and the environment. *Autoimmun Rev,* 9**,** A387-94.

MINDEN, S. L. & SCHIFFER, R. B. 1990. Affective disorders in multiple sclerosis. Review and recommendations for clinical research. *Arch Neurol,* 47**,** 98-104.

MOSTERT, J. P., ADMIRAAL-BEHLOUL, F., HOOGDUIN, J. M., LUYENDIJK, J., HEERSEMA, D. J., VAN BUCHEM, M. A. & DE KEYSER, J. 2008. Effects of fluoxetine on disease activity in relapsing multiple sclerosis: a double-blind, placebo-controlled, exploratory study. *J Neurol Neurosurg Psychiatry,* 79**,** 1027-31.

NOSEWORTHY, J. H., LUCCHINETTI, C., RODRIGUEZ, M. & WEINSHENKER, B. G. 2000. Multiple sclerosis. *N Engl J Med,* 343**,** 938-52.

OO, M. L., CHANG, S. H., THANGADA, S., WU, M. T., REZAUL, K., BLAHO, V., HWANG, S. I., HAN, D. K. & HLA, T. 2011. Engagement of S1P(1)-degradative mechanisms leads to vascular leak in mice. *J Clin Invest,* 121**,** 2290-300.

ORTON, S. M., HERRERA, B. M., YEE, I. M., VALDAR, W., RAMAGOPALAN, S. V., SADOVNICK, A. D. & EBERS, G. C. 2006. Sex ratio of multiple sclerosis in Canada: a longitudinal study. *Lancet Neurol,* 5**,** 932-6.

PARIS, F., FUKS, Z., KANG, A., CAPODIECI, P., JUAN, G., EHLEITER, D., HAIMOVITZ-FRIEDMAN, A., CORDON-CARDO, C. & KOLESNICK, R. 2001. Endothelial apoptosis as the primary lesion initiating intestinal radiation damage in mice. *Science,* 293**,** 293-7.

PATY, D. W. & LI, D. K. 1993. Interferon beta-1b is effective in relapsing-remitting multiple sclerosis. II. MRI analysis results of a multicenter, randomized, double-blind, placebo-controlled trial. UBC MS/MRI Study Group and the IFNB Multiple Sclerosis Study Group. *Neurology,* 43**,** 662-7.

PERSIDSKY, Y., RAMIREZ, S. H., HAORAH, J. & KANMOGNE, G. D. 2006. Blood-brain barrier: structural components and function under physiologic and pathologic conditions. *J Neuroimmune Pharmacol,* 1**,** 223-36.

PHONG, M. C., GUTWEIN, P., KADEL, S., HEXEL, K., ALTEVOGT, P., LINDERKAMP, O. & BRENNER, B. 2003. Molecular mechanisms of L-selectin-induced co-localization in rafts and shedding [corrected]. *Biochem Biophys Res Commun,* 300**,** 563-9.

PLO, I., GHANDOUR, S., FEUTZ, A. C., CLANET, M., LAURENT, G. & BETTAIEB, A. 1999. Involvement of de novo ceramide biosynthesis in lymphotoxin-induced oligodendrocyte death. *Neuroreport,* 10**,** 2373-6.

POLMAN, C. H., O'CONNOR, P. W., HAVRDOVA, E., HUTCHINSON, M., KAPPOS, L., MILLER, D. H., PHILLIPS, J. T., LUBLIN, F. D., GIOVANNONI, G., WAJGT, A., TOAL, M., LYNN, F., PANZARA, M. A. & SANDROCK, A. W. 2006. A randomized, placebo-controlled trial of natalizumab for relapsing multiple sclerosis. *N Engl J Med,* 354**,** 899-910.

POLMAN, C. H., REINGOLD, S. C., BANWELL, B., CLANET, M., COHEN, J. A., FILIPPI, M., FUJIHARA, K., HAVRDOVA, E., HUTCHINSON, M., KAPPOS, L., LUBLIN, F. D., MONTALBAN, X., O'CONNOR, P., SANDBERG-WOLLHEIM, M., THOMPSON, A. J., WAUBANT, E., WEINSHENKER, B. & WOLINSKY, J. S. 2011. Diagnostic criteria for multiple sclerosis: 2010 revisions to the McDonald criteria. *Ann Neurol,* 69**,** 292-302.

PRETORIUS, P. M. & QUAGHEBEUR, G. 2003. The role of MRI in the diagnosis of MS. *Clin Radiol,* 58**,** 434-48.

QIU, H., EDMUNDS, T., BAKER-MALCOLM, J., KAREY, K. P., ESTES, S., SCHWARZ, C., HUGHES, H. & VAN PATTEN, S. M. 2003. Activation of human acid sphingomyelinase through modification or deletion of C-terminal cysteine. *J Biol Chem,* 278**,** 32744-52.

RECKS, M. S., ADDICKS, K. & KUERTEN, S. 2011. Spinal cord histopathology of MOG peptide 35-55-induced experimental autoimmune encephalomyelitis is time- and score-dependent. *Neurosci Lett,* 494**,** 227-31.

REISS, Y., HOCH, G., DEUTSCH, U. & ENGELHARDT, B. 1998. T cell interaction with ICAM-1-deficient endothelium in vitro: essential role for ICAM-1 and ICAM-2 in transendothelial migration of T cells. *Eur J Immunol,* 28**,** 3086-99.

RIBATTI, D., NICO, B., CRIVELLATO, E. & ARTICO, M. 2006. Development of the blood-brain barrier: a historical point of view. *Anat Rec B New Anat,* 289**,** 3-8.

RIVERS, T. M., SPRUNT, D. H. & BERRY, G. P. 1933. Observations on Attempts to Produce Acute Disseminated Encephalomyelitis in Monkeys. *J Exp Med,* 58**,** 39-53.

RIVEST, S. 2009. Regulation of innate immune responses in the brain. *Nat Rev Immunol,* 9**,** 429-39.

RO, H. A. & CARSON, J. H. 2004. pH microdomains in oligodendrocytes. *J Biol Chem,* 279**,** 37115-23.

ROHNELT, R. K., HOCH, G., REISS, Y. & ENGELHARDT, B. 1997. Immunosurveillance modelled in vitro: naive and memory T cells spontaneously migrate across unstimulated microvascular endothelium. *Int Immunol,* 9**,** 435-50.

ROSATI, G. 2001. The prevalence of multiple sclerosis in the world: an update. *Neurol Sci,* 22**,** 117-39.

ROSENMAN, S. J., GANJI, A. A., TEDDER, T. F. & GALLATIN, W. M. 1993. Syn-capping of human T lymphocyte adhesion/activation molecules and their redistribution during interaction with endothelial cells. *J Leukoc Biol,* 53**,** 1-10.

SCHENKEL, A. R., MAMDOUH, Z. & MULLER, W. A. 2004. Locomotion of monocytes on endothelium is a critical step during extravasation. *Nat Immunol,* 5**,** 393-400.

SCHISSEL, S. L., JIANG, X., TWEEDIE-HARDMAN, J., JEONG, T., CAMEJO, E. H., NAJIB, J., RAPP, J. H., WILLIAMS, K. J. & TABAS, I. 1998. Secretory sphingomyelinase, a product of the acid sphingomyelinase gene, can hydrolyze atherogenic lipoproteins at neutral pH. Implications for atherosclerotic lesion development. *J Biol Chem,* 273**,** 2738-46.

SCHISSEL, S. L., SCHUCHMAN, E. H., WILLIAMS, K. J. & TABAS, I. 1996. Zn2+-stimulated sphingomyelinase is secreted by many cell types and is a product of the acid sphingomyelinase gene. *J Biol Chem,* 271**,** 18431-6.

SCHNEIDER-BRACHERT, W., TCHIKOV, V., NEUMEYER, J., JAKOB, M., WINOTO-MORBACH, S., HELD-FEINDT, J., HEINRICH, M., MERKEL, O., EHRENSCHWENDER, M., ADAM, D., MENTLEIN, R., KABELITZ, D. & SCHUTZE, S. 2004. Compartmentalization of TNF receptor 1 signaling: internalized TNF receptosomes as death signaling vesicles. *Immunity,* 21**,** 415-28.

SCHUCHMAN, E. H., LEVRAN, O., PEREIRA, L. V. & DESNICK, R. J. 1992. Structural organization and complete nucleotide sequence of the gene encoding human acid sphingomyelinase (SMPD1). *Genomics,* 12**,** 197-205.

SETO, M., WHITLOW, M., MCCARRICK, M. A., SRINIVASAN, S., ZHU, Y., PAGILA, R., MINTZER, R., LIGHT, D., JOHNS, A. & MEURER-OGDEN, J. A. 2004. A model of the acid sphingomyelinase phosphoesterase domain based on its remote structural homolog purple acid phosphatase. *Protein Sci,* 13**,** 3172-86.

SMITH, B., CARSON, S., FU, R., MCDONAGH, M., DANA, T., CHAN, B. K. S., THAKURTA, S. & GIBLER, A. 2010. *Drug Class Review: Disease-modifying Drugs for Multiple Sclerosis: Final Update 1 Report.* Portland (OR).

SORENSEN, P. S., BERTOLOTTO, A., EDAN, G., GIOVANNONI, G., GOLD, R., HAVRDOVA, E., KAPPOS, L., KIESEIER, B. C., MONTALBAN, X. & OLSSON, T. 2012. Risk stratification for progressive multifocal leukoencephalopathy in patients treated with natalizumab. *Mult Scler,* 18**,** 143-52.

STOFFEL, B., BAUER, P., NIX, M., DERES, K. & STOFFEL, W. 1998. Ceramide-independent CD28 and TCR signaling but reduced IL-2 secretion in T cells of acid sphingomyelinase-deficient mice. *Eur J Immunol,* 28**,** 874-80.

TEICHGRABER, V., ULRICH, M., ENDLICH, N., RIETHMULLER, J., WILKER, B., DE OLIVEIRA-MUNDING, C. C., VAN HEECKEREN, A. M., BARR, M. L., VON KURTHY, G., SCHMID, K. W., WELLER, M., TUMMLER, B., LANG, F., GRASSME, H., DORING, G. & GULBINS, E. 2008. Ceramide accumulation mediates inflammation, cell death and infection susceptibility in cystic fibrosis. *Nat Med,* 14**,** 382-91.

THANNHAUSER S J, R. M. 1940. Studies on animal lipids. XVI. the occurrence of sphingomyelin as a mixture of sphingomyelin fatty acid ester and free sphingomyelin, demonstrated by enzymatic hydrolysis and mild saponification. . *J Biol Chem. ,* 135**,** 1–13.

VAN DIGGELEN, O. P., VOZNYI, Y. V., KEULEMANS, J. L., SCHOONDERWOERD, K., LEDVINOVA, J., MENGEL, E., ZSCHIESCHE, M., SANTER, R. & HARZER, K. 2005. A new fluorimetric enzyme assay for the diagnosis of Niemann-Pick A/B, with specificity of natural sphingomyelinase substrate. *J Inherit Metab Dis,* 28**,** 733-41.

VAN DOORN, R., NIJLAND, P. G., DEKKER, N., WITTE, M. E., LOPES-PINHEIRO, M. A., VAN HET HOF, B., KOOIJ, G., REIJERKERK, A., DIJKSTRA, C., VAN VAN DER VALK, P., VAN HORSSEN, J. & DE VRIES, H. E. 2012. Fingolimod attenuates ceramide-induced blood-brain barrier dysfunction in multiple sclerosis by targeting reactive astrocytes. *Acta Neuropathol,* 124**,** 397-410.

VAN KOOYK, Y., VAN VLIET, S. J. & FIGDOR, C. G. 1999. The actin cytoskeleton regulates LFA-1 ligand binding through avidity rather than affinity changes. *J Biol Chem,* 274**,** 26869-77.

WALTER, S., FASSBENDER, K., GULBINS, E., LIU, Y., RIESCHEL, M., HERTEN, M., BERTSCH, T. & ENGELHARDT, B. 2002. Glycosylation processing inhibition by castanospermine prevents experimental autoimmune encephalomyelitis by interference with IL-2 receptor signal transduction. *J Neuroimmunol,* 132**,** 1-10.

WU, Y. P., MIZUGISHI, K., BEKTAS, M., SANDHOFF, R. & PROIA, R. L. 2008. Sphingosine kinase 1/S1P receptor signaling axis controls glial proliferation in mice with Sandhoff disease. *Hum Mol Genet,* 17**,** 2257-64.

YEDNOCK, T. A., CANNON, C., FRITZ, L. C., SANCHEZ-MADRID, F., STEINMAN, L. & KARIN, N. 1992. Prevention of experimental autoimmune encephalomyelitis by antibodies against alpha 4 beta 1 integrin. *Nature,* 356**,** 63-6.

YU, Z. F., NIKOLOVA-KARAKASHIAN, M., ZHOU, D., CHENG, G., SCHUCHMAN, E. H. & MATTSON, M. P. 2000. Pivotal role for acidic sphingomyelinase in cerebral ischemia-induced ceramide and cytokine production, and neuronal apoptosis. *J Mol Neurosci,* 15**,** 85-97.

ZHANG, Y., LI, X., BECKER, K. A. & GULBINS, E. 2009. Ceramide-enriched membrane domains--structure and function. *Biochim Biophys Acta,* 1788**,** 178-83.

Publications

Based on the PhD experimental work, the following paper is planned to be published:

1. **Davies**, L., Halmer, R., Walter, S., Gulbins, E., Fassbender, K. Inhibition of the acid sphingomyelinase/ceramide system prevents experimental multiple sclerosis. *Manuscript prepared*.

Acknowledgements

First and foremost, I would like to thank my advisors Dr. Silke Walter and Prof. Dr. Klaus Fassbender for their outstanding guidance throughout my thesis. In particular, Dr. Silke Walter was an integral force in the initiation and completion of this work. I would also like to express my sincere gratitude to Dr. Erich Gulbins for his immense knowledge and guidance throughout my research. I would also like to acknowledge Dr Yang Liu for his assistance with technical and theoretical problems.

I would like to also mention my colleagues from the AG Fassbender lab, who made it a joy to come to work every day; in particular, Andrea Schottek and Nadine Commercon who provided technical support and advice. Kan Xie, Xu Liu and Manuela Gries were always there to help and provide assistance when necessary. A special thanks also goes to Ramona Halmer and Sonja Gscheidle who both worked on their medical theses under my supervision with motivation and enthusiasm.

I would also like to acknowledge the help of all the members of the AG Gulbins lab (Institut für Molekularbiologie, Uniklinik Essen, Universität Duisberg/Essen, Germany); in particular, Dr. Brian Henry who was an integral part of our collaborative research, as well as Dr. Katrin Becker-Flegler, Siegfried Moyrer and Regan Henry.

I would like to gratefully acknowledge the financial support for my thesis project from the German Research Foundation (DFG) and Novartis.

Lastly, and most importantly, I offer my sincere gratitude to my family and my family in law for making this an enjoyable and rewarding experience. To them I dedicate this dissertation.